2-2015

Chiral Symmetry Breaking and Chiral Polarization: Tests for Finite Temperature and Many Flavors

Andrei Alexandru
George Washington University

Ivan Horváth
University of Kentucky, ivan.horvath@uky.edu

Chiral Symmetry Breaking and Chiral Polarization: Tests for Finite Temperature and Many Flavors

Digital Object Identifier (DOI)
http://dx.doi.org/10.1016/j.nuclphysb.2014.11.018

Notes/Citation Information
Published in *Nuclear Physics B*, v. 891, p. 1-41.

Available online at www.sciencedirect.com

ScienceDirect

Nuclear Physics B 891 (2015) 1–41

NUCLEAR PHYSICS B

www.elsevier.com/locate/nuclphysb

Chiral symmetry breaking and chiral polarization: Tests for finite temperature and many flavors

Andrei Alexandru [a,*], Ivan Horváth [b]

[a] *The George Washington University, Washington, DC, USA*
[b] *University of Kentucky, Lexington, KY, USA*

Received 4 July 2014; received in revised form 19 November 2014; accepted 20 November 2014

Available online 27 November 2014

Editor: Hubert Saleur

Abstract

It was recently conjectured that, in SU(3) gauge theories with fundamental quarks, *valence* spontaneous chiral symmetry breaking is equivalent to condensation of local dynamical chirality and appearance of chiral polarization scale Λ_{ch}. Here we consider more general association involving the low-energy layer of chirally polarized modes which, in addition to its width (Λ_{ch}), is also characterized by volume density of participating modes (Ω) and the volume density of total chirality (Ω_{ch}). Few possible forms of the correspondence are discussed, paying particular attention to singular cases where Ω emerges as the most versatile characteristic. The notion of *finite-volume "order parameter"*, capturing the nature of these connections, is proposed. We study the effects of temperature (in $N_f = 0$ QCD) and light quarks (in $N_f = 12$), both in the regime of possible symmetry restoration, and find agreement with these ideas. In $N_f = 0$ QCD, results from several volumes indicate that, at the lattice cutoff studied, the deconfinement temperature T_c is strictly smaller than the overlap–valence chiral transition temperature T_{ch} in real Polyakov line vacuum. Somewhat similar intermediate phase (in quark mass) is also seen in $N_f = 12$. It is suggested that deconfinement in $N_f = 0$ is related to indefinite convexity of absolute X-distributions.

* Corresponding author.
E-mail address: aalexan@gwu.edu (A. Alexandru).

http://dx.doi.org/10.1016/j.nuclphysb.2014.11.018

1. Introduction and summary

Eigensystems of Dirac operator in equilibrium gauge backgrounds carry the information on fermionic aspects of quark–gluon dynamics. As an important example, inspection of Dirac spectral representation for scalar fermionic density immediately reveals that spontaneous chiral symmetry breaking (SChSB) is equivalent to mode condensation of massless Dirac operator. Ever since this association has been pointed out [1], it became popular to think about SChSB in terms of quark near-zeromodes.

Contrary to SChSB, the mode condensation property is a well-defined notion in generic quark–gluon system, i.e. even when all quarks are massive. While there is no chiral symmetry of physical degrees of freedom to break in this case, condensing dynamics can still be described via chiral symmetry considerations. Indeed, one can introduce e.g. a pair of fictitious fermionic fields ("valence quarks") of degenerate mass m_v, and cancel their contribution to the action by also adding the associated bosonic partners [2]. This keeps the dynamics of physical quarks and gluons unchanged, but makes it meaningful to consider chiral rotations of valence fields in such extended system, and to inquire about "valence SChSB" in the $m_v \to 0$ limit. In this language,

$$\textbf{vSChSB} \iff \textbf{QMC} \tag{1}$$

i.e. quark mode condensation (QMC) in arbitrary quark–gluon system is equivalent to valence spontaneous chiral symmetry breaking (vSChSB): dynamics supports condensing modes if and only if it supports valence chiral condensate and valence Goldstone pions.

It is useful to think about SChSB in the above more general sense, especially when inquiring about the mechanism underlying the phenomenon [3]. Indeed, the response of massless valence quarks to gauge backgrounds of various quark–gluon systems provides a relevant point of dynamical distinction for associated theories: they either support "broken" or "symmetric" dynamics of the external massless probe. Moreover, valence SChSB is readily observed in lattice simulations with physically relevant flavor arrangements, and the associated dynamical characteristics change smoothly in the light quark regime [3]. Valuable lessons on SChSB can thus be learned by studying its valence version with massive dynamical quarks: vSChSB becomes SChSB as dynamical chiral limit is approached.

Unfortunately, the equivalence of quark mode condensation and valence SChSB does not provide window into specifics of broken quark dynamics. Indeed, the mode condensation property is merely a restatement of symmetry breakdown condition in Dirac spectral representation. However, it was recently proposed that another relation may hold, possibly with similar scope of validity, but with non-trivial dynamical connection to inner workings of the breaking phenomenon [3]. In particular, it was suggested that

$$\textbf{vSChSB} \iff \textbf{DChC} \tag{2}$$

i.e. that valence SChSB is equivalent to *dynamical chirality condensation* (DChC). This offers an intuitively appealing notion that the vacuum effect of chiral symmetry breaking is in fact the phenomenon of chirality condensation. In light of Eq. (1), the above relation carries the same information as QMC–DChC equivalence, which may be preferable for explicit checks.

While entities involved in the above relations will all be defined in Section 2, it should be pointed out now that DChC relates to *dynamical* notion of local chirality in modes [4]: it expresses the tendency for asymmetry in magnitudes of left–right components (local chiral polarization), measured with respect to the baseline of statistical independence. The associated quantifier, the correlation coefficient of polarization $C_A \in [-1, 1]$, is invariant with respect

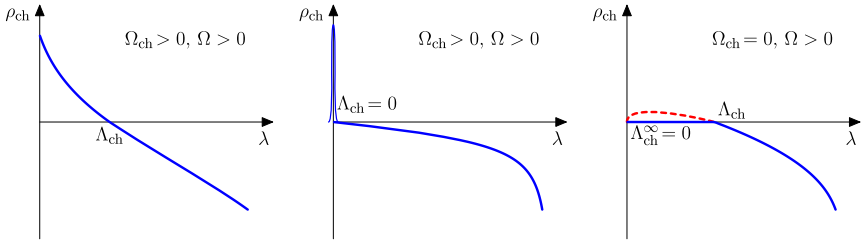

Fig. 1. Layer of chirally polarized modes around $\lambda = 0$ is visible e.g. in the low-energy behavior of $\rho_{ch}(\lambda)$. Standard situation (left) and two singular ones (middle, right) are shown in infinite volume. The dashed segment indicates that infinite volume limit was approached from chirally polarized side. See Section 2.2 for definition of Λ^{∞}_{ch}.

to the choice of parametrization for the asymmetry. It thus provides the information on the quark–gluon system that is inherently dynamical. DChC occurs when near-zeromodes are chirally polarized ($C_A > 0$) and sufficiently abundant, namely when *chiral polarization density* $\rho_{ch}(\lambda) \equiv \rho(\lambda) C_A(\lambda)$ is positive at $\lambda = 0$ in infinite volume.

Important aspect of DChC is that it manifests itself in chiral spectral properties away from strictly infrared limit. Indeed, it was shown [3,4] that mode-condensing theories of physical interest exhibit *chiral polarization scale* Λ_{ch}, marking the spectral point where functions $C_A(\lambda)$, $\rho_{ch}(\lambda)$ change sign and modes become anti-polarized (Fig. 1(left)). The existence of Λ_{ch} in chirally broken asymptotically free theories can be intuitively understood from the fact that free modes are strictly anti-chiral and $C_A(\lambda)$ is thus expected to assume negative values at sufficiently high λ. The simultaneous occurrence of DChC and Λ_{ch} is thus not viewed as accidental but rather generic. This is, in fact, an integral part of the vSChSB–DChC conjecture as formulated in Ref. [3], so that

$$\textbf{vSChSB} \iff \boldsymbol{\Lambda_{\rm ch} > 0} \tag{3}$$

with suitably general definition of Λ_{ch}. Chiral polarization scale can thus be viewed as a non-standard "order parameter" of the breaking phenomenon, and is expected to be naturally tied to the mechanism of SChSB [3].

Relations (2), (3) acquire their full meaning only when the corresponding range of theories is specified. This is relevant since the larger the scope of theories conforming to vSChSB–DChC correspondence, the deeper the connection of local chirality to the symmetry breaking phenomenon. Indeed, if the association is generic, then it must be ascribed to the very nature of quark–gluon interaction. The original vSChSB–DChC conjecture was formulated in the context of SU(3) gauge theories with arbitrary number of fundamental quark flavors of arbitrary masses, and at arbitrary temperature. Thus both broken and symmetric theories are included in this landscape with corresponding transitions providing for most interesting tests of the conjecture. While the maximal range of validity may be significantly larger,[1] this is a physically relevant setup currently associated with the above statements.

The focus of this work involves two main aspects.

(I) In Section 2 we provide more complete description of chiral polarization phenomenon, and formulate the proposed connections to vSChSB within such wider context. Refined description reflects the premise that the vacuum feature we are associating with vSChSB is the layer of

[1] For example, extension to general SU(N) gauge groups may hold as well.

chirally polarized modes around $\lambda = 0$ ("surface of the Dirac sea"). Apart from its width (Λ_{ch}), global characterization of this structure also includes volume density of modes involved (Ω), and the volume density of total chirality generated by them (Ω_{ch}). Incorporating these characteristics allows us to distinguish and discuss various special/singular cases that might arise. For example, the layer could approach zero width in the infinite volume limit, but acquire sufficiently singular abundance of modes so as to generate positive Ω_{ch} and Ω (see Fig. 1(middle)). Another possibility is that polarization density asymptotically vanishes on the layer, due to modes being concentrated on a subset of space–time with measure zero, but Ω remains positive in the infinite volume limit. This is schematically shown in Fig. 1(right). Even if behaviors of the above type won't appear in target continuum theories, they are likely to show up at low lattice cutoffs. Working within a framework capturing such cases is beneficial to make the proposed connections as universal as possible.

Related to the above is a suggestion, described in Section 2.4, whose conceptual content goes beyond that in Ref. [3]. To convey this, note that our discussion implicitly proceeded in infinite volume where the notions of condensate and symmetry breaking are defined. For example, the generic form of relation (3) in the extended framework (see Conjecture 2″) is

$$\textbf{vSChSB} \iff \boldsymbol{\Omega > 0} \tag{3′}$$

implying that appearance of chirally polarized layer around the surface of Dirac sea is considered to be physically significant if $\Omega \equiv \lim_{V\to\infty} \Omega(V) > 0$. Theories without polarized low modes in large finite volumes ($\Omega(V)$ identically zero) are then predicted to be unbroken, but theories with polarized low modes ($\Omega(V) > 0$) could also be unbroken if $\lim_{V\to\infty} \Omega(V) = 0$. Consistently with available data, we propose in Conjecture 3 that the latter possibility does not occur: if large-volume dynamics generates chiral polarization in low end of the spectrum, then valence chiral condensate appears in the infinite volume limit and vice versa. This provides for the closest possible relationship between vSChSB and chiral polarization (ChP), and it is in this sense that we refer to Λ_{ch}, Ω_{ch} and Ω as *finite-volume "order parameters"*.[2] In this context, the correspondence analogous to (2) is expressed as

$$\textbf{vSChSB} \iff \textbf{ChP} \text{ in large finite volumes} \tag{2′}$$

and the right-hand side of relation (3′) modifies to: $\Omega(V) > 0$ for $V_0 < V < \infty$.

(II) We present new lattice data supporting the above ideas. It is known that, at zero temperature, $N_f = 0$ theory [3,4] as well as $N_f = 2 + 1$ theory at physical point [3] exhibit chiral polarization, in accordance with the presence of vSChSB, and thus with the proposed equivalence. There is also an initial evidence that subjecting $N_f = 0$ QCD to thermal agitation, chiral polarization and vSChSB cease to exist at common temperature T_{ch} [3]. When contemplating the validity of the vSChSB–ChP relationship over the vast theory landscape considered, it is useful to think of $N_f = 0$, $T = 0$ theory as a reference point [3]. Indeed, this dynamics produces maximal breaking of valence chiral symmetry, with thermal effects and the effects of light dynamical quarks providing two possible routes to symmetry restoration. Thus, in pilot investigations, it is natural to examine these two deformations of quenched theory independently of one another, both to ascertain conjecture's validity in such instances, as well as to learn about specific features associated with the two qualitatively different effects. This work is the first step in that direction

[2] As discussed in Section 2.4, Λ_{ch}, Ω_{ch} and Ω are zero/non-zero simultaneously in finite volume: they effectively represent a single finite-volume order parameter.

with finite-temperature aspect examined in Section 3, and many-flavor dynamics in Section 4. All of our results are consistent with the vSChSB–ChP equivalence.

Few noteworthy byproducts of our main inquiry are also discussed here. (i) Performing a volume analysis at the lattice cutoff studied, we show the existence of the (lattice) phase $T_c < T < T_{ch}$ in $N_f = 0$, simultaneously exhibiting vSChSB and deconfinement [14,12,13]. This chiral polarization dynamics appears to be of the singular type ($\Lambda_{ch} = 0, \Omega_{ch} > 0, \Omega > 0$). (ii) One of the characteristic features of the above "mixed phase" is the appearance of very inhomogeneous near-zeromodes, well distinguished from the bulk of the spectrum. We find an intermediate phase (in quark mass) with such properties also in $N_f = 12$. The relevance of these phases for continuum physics remains an open issue in both cases. (iii) Elementary analysis of the detailed chiral polarization characteristic, namely absolute X-distribution, is also performed. Among other things, our data in $N_f = 0$ indicate that deconfinement is characterized by the appearance of distributions with indefinite convexity.

2. The background and the conjectures

We start by reviewing the relevant background, and formulating the connections we aim to test. Our discussion will be fairly detailed and self-contained, in part to sufficiently extend pertinent parts of article [3] which were necessarily rather brief. In addition, we build an extended formalism for description of chiral polarization, which allows us to include special/singular behaviors and has some benefits for continuum-limit considerations.

2.1. Valence chiral symmetry and mode condensation

Implicitly assumed in what follows is the setup involving SU(3) gluons interacting with N_f fundamental quarks of masses $M = (m_1, m_2, \ldots, m_{N_f})$. To formally include valence chiral symmetry considerations, the system is augmented by a pair of degenerate valence quarks of mass m_v, and a pair of complex commuting fields (pseudofermions) compensating for the dynamical effect of these fictitious particles [2]. This schematically corresponds to the action,

$$S = S_g + \sum_{f=1}^{N_f} \bar{\psi}_f (D_{(1)} + m_f)\psi_f + \sum_{i=1}^{2} \bar{\eta}_i (D_{(2)} + m_v)\eta_i + \sum_{i=1}^{2} \phi_i^\dagger (D_{(2)} + m_v)\phi_i \tag{4}$$

where S_g is the pure glue contribution. When viewing the above as expression in the continuum, then $D_{(1)} = D_{(2)} = D$, namely the continuum Dirac operator. However, on the lattice it is possible, and sometimes desirable, to consider different discretizations for dynamical and valence quarks. In particular, the role of $D_{(2)}$ in our case is to describe the response of physical vacuum to external chiral probe. It is thus desirable that it provides for exact lattice chiral symmetry, even though some numerically cheaper $D_{(1)}$ could have been used to simulate physical quarks and to define the theory.

Flavored chiral rotations of valence quark fields in the above extended system become the symmetry of the action in the $m_v \to 0$ limit, and one can meaningfully ask whether this symmetry is broken by the vacuum. If so, we speak of *valence chiral symmetry breaking* (vSChSB). It has the usual consequence of being associated with the triplet of massless valence pions. While these are not physical states, they express the ability of the physical vacuum to support a specific type of long range order: the same kind of order that is required for physical chiral symmetry to

be broken in the dynamical massless limit. vSChSB is thus a relevant vacuum characteristic of QCD-like theories.

Following the steps involved in derivation of the standard Banks–Casher relation [1], one can inspect that the valence chiral condensate in theory (4) is given by

$$\Sigma(M) \equiv \lim_{m_v \to 0} \lim_{V \to \infty} \langle \bar{\eta}\eta \rangle_{M, m_v, V} = \pi \lim_{\epsilon \to 0^+} \frac{1}{\epsilon} \lim_{V \to \infty} \sigma_{(2)}(\epsilon, M, V) \tag{5}$$

where η is one (arbitrary) of the valence flavors, $\sigma_{(2)} = \sigma_{(2)}(\lambda, M, V)$ the cumulative eigenmode density of $D_{(2)}$ and V the 4-volume. In the continuum, $\sigma_{(2)} \to \sigma$ is the cumulative eigenmode density of continuum Dirac operator. On the lattice, we implicitly assume that $D_{(2)}$ is the overlap Dirac operator [5] which is our discretization of choice in this study, and for which the relation such as (5) can be straightforwardly derived [6].

The notion of *cumulative eigenmode density*, used above, is defined as

$$\sigma(\lambda, M, V) \equiv \frac{1}{V} \left\langle \sum_{0 \le \lambda_k < \lambda} 1 \right\rangle_{M, V} \tag{6}$$

where λ (real number) represents the imaginary part of Dirac eigenvalue. In case of overlap Dirac operator one can also take it to be the magnitude of the eigenvalue multiplied by the sign of the imaginary part. λ_k are the values associated with given gauge background and ordered appropriately. Note that $\sigma(\lambda, M, V) \equiv 0$ for $\lambda \le 0$. The differential version of σ, referred to as *eigenmode density*, is generally available and frequently useful, namely

$$\rho(\lambda, M, V) \equiv \lim_{\epsilon \to 0^+} \frac{\sigma(\lambda + \epsilon, M, V) - \sigma(\lambda, M, V)}{\epsilon} = \frac{\partial}{\partial_+ \lambda} \sigma(\lambda, M, V) \tag{7}$$

Note that we chose to distinguish the above eigenmode density from the usual

$$\bar{\rho}(\lambda, M, V) \equiv \frac{1}{V} \sum_k \left\langle \delta(\lambda - \lambda_k) \right\rangle_{M, V} \tag{8}$$

which, in some singular cases, has to be represented by a generalized function with at most countably many "atoms" (δ-functions), while ρ is always an ordinary function which simply takes the value "∞" at the position of the atoms.

The infinite volume limit of $\rho(\lambda, M, V)$ will be defined as

$$\rho(\lambda, M) \equiv \frac{\partial}{\partial_+ \lambda} \lim_{V \to \infty} \sigma(\lambda, M, V) \tag{9}$$

rather than as pointwise limit of $\rho(\lambda, M, V)$, but the two can only differ in certain singular points of the spectrum. The theory is said to exhibit *quark mode condensation* (QMC) if

$$\lim_{\epsilon \to 0^+} \frac{1}{\epsilon} \lim_{V \to \infty} \sigma(\epsilon, M, V) = \rho(0, M) > 0 \tag{10}$$

i.e. when the abundance of "infinitely infrared" modes scales as the total number of modes, namely with space–time volume. Relation (5) then implies

$$\Sigma(M) > 0 \iff \rho(0, M) > 0 \tag{1'}$$

which is an explicit representation of equivalence (1) between vSChSB and QMC.

Few remarks regarding the above should now be made.

(i) The discussion has been carried out at a rather general level mainly to accommodate the possibility of most singular behavior at the origin in the infinite volume limit. If $\lambda = 0$ is the only "atom" in that situation, then $\bar{\rho}(\lambda, M) = C(M)\delta(\lambda) + \hat{\rho}(\lambda, M)$, with $\hat{\rho}$ being an ordinary function, and $C(M) = \lim_{\epsilon\to 0} \int_0^\epsilon \bar{\rho}(\lambda, M)\, d\lambda$. We then have

$$\rho(0, M) = \lim_{\epsilon\to 0^+} \frac{C(M)}{\epsilon} + \lim_{\lambda\to 0^+} \rho(\lambda, M) \tag{11}$$

since $\lim_{\lambda\to 0^+} \hat{\rho}(\lambda, M) = \lim_{\lambda\to 0^+} \rho(\lambda, M)$. Therefore, in addition to the usual second term, mode condensate acquires an infinite value if there is an atom of spectral mode density at the origin.[3] This is in accordance with diverging chiral condensate in such instance, namely

$$\Sigma(M) = \lim_{m_v\to 0} \frac{2C(M)}{m_v} + \pi \lim_{\lambda\to 0^+} \rho(\lambda, M) \tag{12}$$

We emphasize that the singular accumulation of modes discussed above is not due to exact zero-modes of finite volumes: their contribution is well known to vanish in the infinite volume limit. Rather, $C(M) > 0$ would have to be generated by modes that are "squeezed" into near-zeromodes at arbitrary finite volume but become "infinitely infrared" as volume is taken to infinity. It is not known whether there are continuum theories generating such dynamics, but we will discuss the behavior that might be of this type at finite cutoff.

(ii) It should be noted that, at finite cutoff, it is in principle possible to obtain contradictory answers on vSChSB (QMC) with different choices of $D_{(2)}$. However, such discrepancies, if any, are expected to disappear sufficiently close to the continuum limit.

(iii) In the above considerations we assumed $T = 0$ for simplicity. Incorporating theories on 3-volume V_3 at finite temperature T is straightforward and simply involves replacing $V \to (T, V_3)$ in labels, and $V \to V_3/T$ in volume factors.

2.2. *Spectral measures of dynamical chirality*

The term "*dynamical local chirality*" refers to characterization of local asymmetry in left–right values of Dirac eigenmodes using absolute polarization method of Ref. [4]. Dynamical nature of this approach mainly stems from the fact that it quantifies polarization relative to the population of statistically independent left–right components. The basic characteristic is the correlation coefficient of polarization $C_A \in [-1, 1]$, assigned to a given eigenmode ψ_λ. It is linearly related to the probability that the local value of ψ_λ is more polarized than value chosen from associated distribution of statistically independent left–right components. In case of correlation ($C_A > 0$), dynamics enhances polarization and the mode is referred to as chirally polarized, while anti-correlation ($C_A < 0$) indicates that dynamics suppresses polarization and the mode is chirally anti-polarized. Such comparison of polarization can also be performed in a detailed differential manner, resulting in absolute X-distribution $P_A(X)$, with $X \in [-1, 1]$. A concise introduction to these concepts together with precise definitions can be found in Appendix A.

Spectral characteristics of a given theory based on dynamical chirality measures C_A and $P_A(X)$ can be defined as follows [3]. The cumulative dynamical chirality per unit volume (*cumulative chiral polarization density*), is given by

[3] Note that $\rho(0, M)$ can in principle be infinite even when $C(M) = 0$ since $\hat{\rho}(\lambda)$ could still have an ordinary integrable divergence at $\lambda = 0$.

$$\sigma_{ch}(\lambda, M, V) \equiv \frac{1}{V}\left\langle \sum_{0\leq\lambda_k<\lambda} C_{A,k} \right\rangle_{M,V} \tag{13}$$

where $C_{A,k}$ is chiral polarization (correlation) in the k-th mode. The associated differential contribution due to modes at scale λ, namely

$$\rho_{ch}(\lambda, M, V) \equiv \lim_{\epsilon\to 0^+} \frac{\sigma_{ch}(\lambda+\epsilon, M, V) - \sigma_{ch}(\lambda, M, V)}{\epsilon} = \frac{\partial}{\partial_+\lambda}\sigma_{ch}(\lambda, M, V) \tag{14}$$

is referred to as *chiral polarization density* as is its formal companion

$$\bar{\rho}_{ch}(\lambda, M, V) \equiv \frac{1}{V}\sum_k \left\langle \delta(\lambda-\lambda_k) C_{A,k} \right\rangle_{M,V} \tag{15}$$

which has to be represented by a generalized function in certain singular cases.

The average chiral polarization at scale λ is given by

$$C_A(\lambda, M, V) \equiv \lim_{\epsilon\to 0^+} \frac{\sigma_{ch}(\lambda+\epsilon, M, V) - \sigma_{ch}(\lambda, M, V)}{\sigma(\lambda+\epsilon, M, V) - \sigma(\lambda, M, V)} = \frac{\rho_{ch}(\lambda, M, V)}{\rho(\lambda, M, V)} \tag{16}$$

where the second equation only applies when $0 < \rho(\lambda, M, V) < \infty$. We similarly define the average absolute X-distribution at scale λ which, written without shorthands, reads

$$P_A(X, \lambda, M, V) \equiv \lim_{\epsilon\to 0^+} \frac{\langle \sum_{\lambda\leq\lambda_k<\lambda+\epsilon} P_{A,k}(X)\rangle_{M,V}}{\langle \sum_{\lambda\leq\lambda_k<\lambda+\epsilon} 1\rangle_{M,V}} \tag{17}$$

where $P_{A,k}(X)$ is the absolute X-distribution of the eigenmode associated with λ_k.

The infinite volume limit of $\rho_{ch}(\lambda, M, V)$ is defined to be

$$\rho_{ch}(\lambda, M) \equiv \frac{\partial}{\partial_+\lambda} \lim_{V\to\infty} \sigma_{ch}(\lambda, M, V) \tag{18}$$

We say that the theory exhibits *dynamical chirality condensation* [3] if

$$\lim_{\epsilon\to 0^+} \frac{1}{\epsilon} \lim_{V\to\infty} \sigma_{ch}(\epsilon, M, V) = \rho_{ch}(0, M) > 0 \tag{19}$$

i.e. if its "infinitely infrared" Dirac modes are chirally polarized and their contribution to dynamical chirality scales with space–time volume. Similarly, dynamical anti-chirality condensation occurs when $\rho_{ch}(0, M) < 0$. Note that (anti-)chirality condensation implies mode condensation but not vice-versa.

Since $\rho_{ch}(\lambda)$ is a real-valued function of indefinite sign, we can assign *chiral polarization scale* $\Lambda_{ch} \geq 0$ to it as the largest Λ such that $\rho_{ch}(\lambda) > 0$ on $[0, \Lambda)$ except for isolated zeros. The provision for "isolated zeros" has two rationales. First, even with such zeros present, Λ_{ch} retains its intended meaning as a spectral range of dynamical chirality around the surface of Dirac sea. Second, it ensures that defining chiral polarization scale via $C_A(\lambda)$ leads to the same scale in finite volume. Indeed, if $\Lambda'_{ch} \geq 0$ is the largest Λ such that $C_A(\lambda) > 0$ on $[0, \Lambda)$ except for isolated zeros, then $\Lambda_{ch} = \Lambda'_{ch}$ in finite volume.[4] Note that when positive Λ_{ch} doesn't exist, the above definition is vacuously true for $\Lambda_{ch} = 0$, which is then the assigned chiral polarization scale. Also, $\Lambda_{ch} = \infty$ is associated with $\rho_{ch}(\lambda)$ that is positive on $[0, \infty)$ except for possible

[4] What is relevant here is that a zero of C_A is also a zero of ρ_{ch} but not necessarily vice-versa.

isolated zeros. Given $\Lambda_{ch} = \Lambda_{ch}(M, V)$, the *total dynamical chirality* of Dirac spectrum at low energy $\Omega_{ch} = \Omega_{ch}(M, V)$ is

$$\Omega_{ch} \equiv \max\Big\{\sigma_{ch}(\Lambda_{ch}),\ \lim_{\epsilon\to 0^+} \sigma_{ch}(\Lambda_{ch}+\epsilon)\Big\} \tag{20}$$

where the possibility of discontinuity at Λ_{ch} has been taken into account. The associated *total number of chirally polarized modes* $\Omega = \Omega(M, V)$ is

$$\Omega \equiv \begin{cases} \sigma(\Lambda_{ch}) & \text{if } \Omega_{ch} = \sigma_{ch}(\Lambda_{ch}) \\ \lim_{\epsilon\to 0^+} \sigma(\Lambda_{ch}+\epsilon) & \text{if } \Omega_{ch} = \lim_{\epsilon\to 0^+} \sigma_{ch}(\Lambda_{ch}+\epsilon) \end{cases} \tag{21}$$

Note that the characteristics $\Omega \geq 0$, $\Omega_{ch} \geq 0$ are volume densities while the condensates $\rho(0)$, $\rho_{ch}(0)$ are both volume and spectral densities.

Infinite volume limits of the above objects require some attention since the order of operations might be relevant in certain cases. In discussion of the condensation phenomena, we emphasized the primary role of cumulative densities, with their infinite volume limits

$$\sigma(\lambda, M) \equiv \lim_{V\to\infty} \sigma(\lambda, M, V) \qquad \sigma_{ch}(\lambda, M) \equiv \lim_{V\to\infty} \sigma_{ch}(\lambda, M, V) \tag{22}$$

being the basis for computation of the condensates. However, one virtue of chiral polarization framework is that such insistence on the order of operations ceases to be crucial. In fact, our default view of infinite volume limits for Λ_{ch}, Ω and Ω_{ch} is just the direct limit of their finite-volume versions, rather than corresponding functionals of $\sigma_{ch}(\lambda, M)$ and $\sigma(\lambda, M)$. Thus, while we explicitly distinguish the two options, for example

$$\Omega_{ch}(M) \equiv \lim_{V\to\infty} \Omega_{ch}(M, V) \qquad \Omega_{ch}^{\infty}(M) \equiv \Omega_{ch}\big[\sigma_{ch}(\lambda, M)\big] \tag{23}$$

it is the first definition that is implicitly understood if not stated otherwise. We use analogous notational convention also in case of Λ_{ch} and Ω.

Few remarks regarding these concepts should be made.

(i) The above definitions of Λ_{ch} and Ω_{ch} assume certain analytic properties of $\sigma_{ch}(\lambda)$, such as existence of $\rho_{ch}(\lambda)$ or the limit in Eq. (20). In case of cumulative mode density $\sigma(\lambda)$, such properties are, for most part, inherent in its definition, i.e. it is continuous except possibly at countably many finite jumps, and differentiable almost everywhere. While these properties are expected to hold also for $\sigma_{ch}(\lambda)$ in any theory, it is comforting that Λ_{ch} and Ω_{ch} can be assigned to $\sigma_{ch}(\lambda)$ that is completely generic. The corresponding definition and related considerations are discussed in Appendix B.

(ii) In terms of $\sigma_{ch}(\lambda)$, chiral polarization scale corresponds to the largest Λ such that $\sigma_{ch}(\lambda)$ is strictly increasing on $[0, \Lambda]$, and Ω_{ch} its associated maximal value. Fig. 2 shows various behaviors of $\sigma_{ch}(\lambda)$, illustrating how Λ_{ch} and Ω_{ch} are assigned via above definitions. For the current purpose, one should only view $\sigma_{ch}(\lambda)$, $\rho_{ch}(\lambda)$ shown as admissible pairs of functions: many of these situations are not expected to occur in theories of interest.

(iii) In the above considerations we assumed $T = 0$ for notational simplicity. Extension of all definitions to finite temperatures is straightforward (see remark (iii) of Section 2.1).

2.3. *Conjecture formulations*

We will consider and extend Conjecture 2 of Ref. [3], which ties the phenomenon of valence spontaneous chiral symmetry breaking to that of dynamical local chirality in low-lying modes.

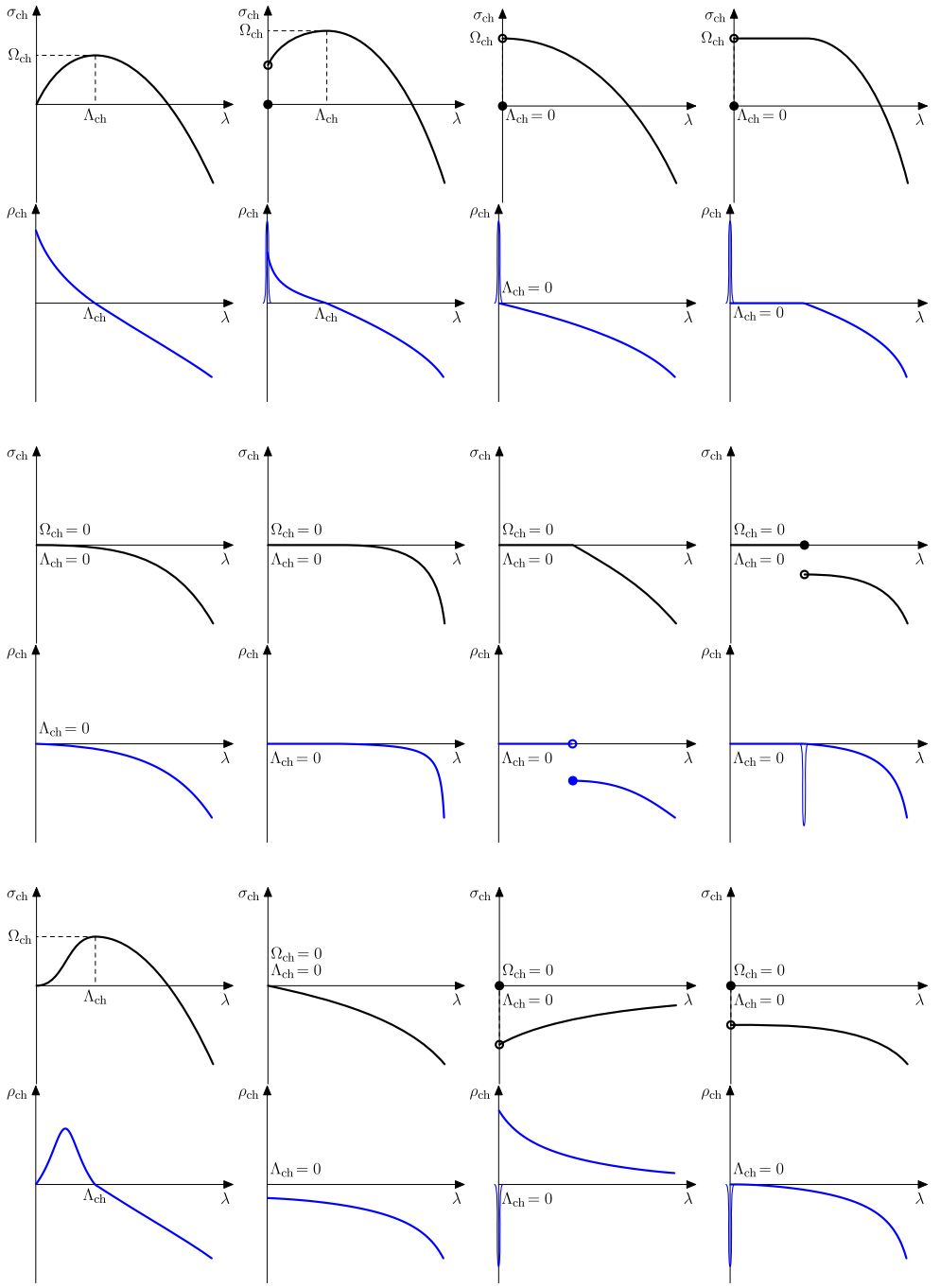

Fig. 2. Examples of assigning Λ_{ch} and Ω_{ch} to $\sigma_{ch}(\lambda)$. The associated $\rho_{ch}(\lambda)$ is shown in the lower figure for each case. For theory in *infinite volume*, Conjecture 2′ identifies the first/second pair of rows as options that can only occur in broken/symmetric vacuum, while the behavior in the third pair of rows is predicted to be impossible for theories in $\mathcal{T}$. The possibilities in each category are not meant to be exhaustive or guaranteed to occur.

Such vSChSB–DChC correspondence was proposed to hold over the set $\mathcal{T}$ containing SU(3) gauge theories in $3+1$ space–time dimensions with any number (N_f) of fundamental quarks of arbitrary masses $M \equiv (m_1, m_2, \ldots, m_{N_f})$, and at arbitrary temperature T. Different continuum theories are thus labeled by (M, T). Statements of this section are formulated in infinite volume (infinite extent of all spatial dimensions) so that spontaneous symmetry breaking and the condensation concepts have definite meaning. To begin with, we formulate Conjecture 2 using more precise language and concepts developed here. By "chiral polarization characteristics" we mean the parameters Λ_{ch}, Λ_{ch}^{∞}, Ω_{ch}, Ω_{ch}^{∞}, Ω, Ω^{∞}.

Conjecture 2. *The following holds in every lattice-regularized $(M, T) \in \mathcal{T}$ at sufficiently large ultraviolet cutoffs Λ_{lat} and infinite volume.*

(I) *Chiral polarization characteristics exist and are zero or non-zero simultaneously. Moreover, $\Lambda_{ch} = \Lambda_{ch}^{\infty}$ and $0 \leq \Lambda_{ch} \ll \Lambda_{lat}$. If $\Lambda_{ch} > 0$ then $\rho_{ch}(\lambda)$ is positive on $[0, \Lambda_{ch})$.*

(II) *The property of valence spontaneous chiral symmetry breaking is characterized by*

$$\Sigma > 0 \iff \rho(\lambda = 0) > 0 \iff \Lambda_{ch} > 0 \tag{24}$$

(III) *$\rho_{ch}(\lambda)$ is non-positive for $\lambda > \Lambda_{ch}$, except possibly in the vicinity of Λ_{lat}.*

The statement is thus split into three parts which we now discuss.

(I) $\Lambda_{ch} = \Lambda_{ch}^{\infty}$ implies that $\Omega_{ch} = \Omega_{ch}^{\infty}$ and $\Omega = \Omega^{\infty}$. Neither this pairwise equality nor the simultaneous positivity of all six parameters follows from definitions alone. Rather, they represent anticipated constraints on actual dynamical behavior in theories under consideration close to the continuum. Note that the statement rules out the possibility of chiral polarization over the whole Dirac spectrum. Also, while $\Lambda_{ch} > 0$ implies positivity of $\rho_{ch}(\lambda)$ on $[0, \Lambda_{ch})$ only up to isolated points, such points are not expected to be present in infinite volume, as explicitly stated.

(II) Relation (24) asserts that chiral polarization scale Λ_{ch} is an unconventional order parameter of vSChSB on $\mathcal{T}$: chiral symmetry is broken if and only if this dynamical scale is generated. Note that from (I) and (II) it follows that $\rho(0) > 0 \Leftrightarrow \rho_{ch}(0) > 0$, which is the mathematical representation of relation (2): quark mode condensation (hence vSChSB) is equivalent to dynamical chirality condensation. Anti-chirality doesn't condense [3].

(III) This part reflects the expectation that dynamical chirality can only occur in the low end of the Dirac spectrum, characterized by Λ_{ch}. In lattice theory, chiral polarization could exist in the vicinity of the cutoff (due to lattice artifacts) but will scale out in the continuum limit. While generic anti-chirality in the ultraviolet is supported by asymptotic freedom, the assertion that chiral polarization cannot dominate at intermediate scales, i.e. in a spectral band separated from origin, is not easy to verify directly. Indeed, reaching such intermediate parts of Dirac spectra via numerical lattice QCD sufficiently close to the continuum limit can be computationally demanding. Nevertheless, at least at zero temperature, there is little doubt that the above scenario holds since running of the gauge coupling, well understood, is monotonic across scales. The situation at finite temperature is more involved though. The effects of asymmetry between magnetic and electric couplings [8] and the influence of infrared fixed point in dimensionally reduced (3-d) theory [9] could improve prospects for more complicated behavior at sufficiently high temperatures. However, the available data is not hinting the existence of intermediate-scale chirality, as reflected in the statement.

The meaning of Conjecture 2 is directly tied to the lattice definition of the theory: following some line of constant physics in the parameter space of a regularized setup, it is claimed that the statement becomes valid in associated lattice theories with sufficiently large cutoff.[5] It is thus useful to attempt a formulation of the vSChSB $\leftrightarrow$ DChC correspondence valid for the widest range of cutoffs possible. Similarly to vSChSB $\leftrightarrow$ QMC connection, which holds at arbitrary cutoff, the range of validity may include even symmetry breaking instances due to lattice artifacts. To formulate the alternative version of the conjecture, we were mostly guided by results of the numerical study at finite temperature, described in Section 3. These results suggest the viability of the scenario in which chirally broken dynamics generates chiral polarization only via discrete contribution from strictly infrared modes. To incorporate these cases, it is necessary to abandon the notion that chiral polarization characteristics are non-zero simultaneously. Conjecture 2′ stated below provides for the minimal extension of this type.

Conjecture 2′. *The following holds in every lattice-regularized* $(M, T) \in \mathcal{T}$ *at sufficiently large ultraviolet cutoffs* Λ_{lat} *and infinite volume.*

(I) *Chiral polarization characteristics exist,* $\Lambda_{ch} = \Lambda_{ch}^{\infty}$ *and* $0 \leq \Lambda_{ch} \ll \Lambda_{lat}$. *If* $\Lambda_{ch} > 0$ *then* $\rho_{ch}(\lambda)$ *is positive on* $[0, \Lambda_{ch})$.

(II) *The property of valence spontaneous chiral symmetry breaking is characterized by*

$$\Sigma > 0 \iff \rho(\lambda = 0) > 0 \iff \Omega_{ch} > 0 \tag{24′}$$

(III) $\rho_{ch}(\lambda)$ *is non-positive for* $\lambda > \Lambda_{ch}$, *except possibly in the vicinity of* Λ_{lat}.

Discussion following Conjecture 2 mostly applies here as well but it is Ω_{ch} that serves as the order parameter of vSChSB on $\mathcal{T}$: chiral symmetry is broken if and only if total low-energy chirality per unit volume is non-zero. Singular cases motivating this extension arise when positive core in $\rho_{ch}(\lambda, V)$ becomes proportional to $\delta(\lambda)$ in the infinite volume limit, leading to $\Lambda_{ch} = 0$, $\Omega_{ch} > 0$ as shown in Fig. 1(middle).[6] Note that vSChSB $\leftrightarrow$ DChC correspondence still follows from (I) and (II). Part (III) implies that Ω_{ch} is not just the total low-energy chirality but the total chirality of the entire Dirac spectrum. The essential content of Conjecture 2′ can then be summarized by saying that quark–gluon dynamics breaks chiral symmetry if and only if it generates volume density of dynamical chirality.

It is interesting to look back at Fig. 2 in light of the above statement. Indeed, assuming that various $\sigma_{ch}(\lambda)$, $\rho_{ch}(\lambda)$ shown represent infinite volume limits, the first pair of rows corresponds to options for chirally broken vacuum, the second pair is associated with symmetric vacuum, and the cases in the third pair do not occur on $\mathcal{T}$ if Conjecture 2′ is valid.

With the same rationale that motivated Conjecture 2′, we now put forward yet more generic association of chiral polarization and vSChSB. In particular, it is possible to drop the notion that DChC is a necessary companion of vSChSB, while still maintaining the connection to chiral polarization. This can arise when, in addition to simultaneous positivity, the pairwise equality of chiral polarization parameters is abandoned as well. The prototypical situation we have in mind is when $\Lambda_{ch}(V) > 0$ converges to $\Lambda_{ch} > 0$ in the infinite volume limit, but $\rho_{ch}(\lambda, V)$ scales to zero

[5] In the continuum language, masses $M \equiv (m_1, m_2, \ldots, m_{N_f})$ label different continuum theories (different lines of constant physics) and should thus be viewed as renormalized quark masses in some fixed scheme.

[6] The possibility of transition from Λ_{ch} to Ω_{ch} has been discussed in Ref. [3] already. However, Ω_{ch} was denoted as Ω in that work.

on interval $[0, \Lambda_{ch})$. This results in $\Lambda_{ch}^{\infty} = 0$ and $\Omega_{ch} = 0$ (see Fig. 1(right)). Note that $\rho_{ch} = \rho C_A$ can approach zero due to *(i)* $C_A \to 0$ or *(ii)* $\rho \to 0$ or *(iii)* both. Option *(i)* is quite interesting since it can occur when low-lying Dirac modes are dimensionally reduced.[7] Indeed, the "active" part of the eigenmode can be chirally polarized and induce vSChSB, but its contribution to total polarization gets overwhelmed by the uncorrelated bulk in the infinite volume limit. While $\Omega_{ch} = 0$ in this situation, $\Omega > 0$ still signals the association of chiral symmetry breaking and chiral polarization. Thus, in the form below, the conjecture states that vSChSB proceeds if and only if there is a volume density of chirally polarized modes around the surface of the Dirac sea.

Conjecture 2″. *The following holds in every lattice-regularized* $(M, T) \in \mathcal{T}$ *at sufficiently large ultraviolet cutoffs* Λ_{lat} *and infinite volume.*

(I) *Chiral polarization characteristics exist and* $0 \leq \Lambda_{ch} + \Lambda_{ch}^{\infty} \ll \Lambda_{lat}$.
(II) *The property of valence spontaneous chiral symmetry breaking is characterized by*

$$\Sigma > 0 \iff \rho(\lambda = 0) > 0 \iff \Omega > 0 \tag{24″}$$

(III) $\rho_{ch}(\lambda)$ *is non-positive for* $\lambda > \Lambda_{ch}^{\infty}$, *except possibly in the vicinity of* Λ_{lat}.

It should be emphasized that all three versions of the conjecture may be valid simultaneously. Indeed, they do not necessarily exclude one another, but rather express varied degrees of detail in which chiral polarization could manifest itself in vSChSB. In fact, it is entirely feasible that the differences are only relevant at sufficiently low lattice cutoffs.

2.4. Finite volume

Discussion in the previous section has been carried out in the infinite volume which is a native setting for vSChSB and various condensates. However, it is both relevant practically and interesting conceptually, to examine how chiral polarization concepts enter the finite volume considerations.

To begin with, it is useful to fix a convention regarding exact zeromodes. Indeed, the default lattice setup in this discussion involves standard (anti-)periodic boundary conditions and the overlap Dirac operator as a chiral probe. Consequently, exact zeromodes can appear in finite volume whether infinite-volume theory breaks chiral symmetry or not. In either case though, their abundance doesn't scale with volume. This renders them inessential for valence condensate and there is a choice whether to include them in specific considerations. For our purposes it is more convenient to leave zeromodes out which is what will be assumed from now on in this article. In fact, one useful advantage of using overlap operator is that it cleanly separates out topological modes, ensuring that their *a priori* local chirality doesn't contaminate that of near-zeromodes which are of actual interest.

The definition of chiral symmetry breaking in Dirac eigenmode representation involves a strictly infrared condition: the existence of mode condensate (QMC). This is of course not surprising: the strictly infrared nature of relevant mass ($m_v = 0$) gets translated into strictly infrared corner of the Dirac spectrum ($\lambda = 0$). However, applying QMC condition to detect vSChSB in finite volume is futile since it is never satisfied. Indeed, $\rho(\lambda \to 0, V)$ is zero identically. This is

[7] Loosely speaking, eigenmodes are *dimensionally reduced* when their effective support comprises a vanishing fraction of the associated domain in the infinite-volume limit.

symptomatic of the fact that vSChSB $\leftrightarrow$ QMC correspondence is kinematic in nature: since the definition of vSChSB demands infinite volume, QMC condition, being its equivalent, reacts to avoid conflict with the presence of infrared cutoff.

However, if the mechanism of vSChSB was known, it would be reasonable to expect that other properties of quark modes, those suggested by the mechanism, could be used to signal vSChSB even in given finite volume. After all, broken and symmetric dynamics should be distinguishable in any volume. In fact, if infrared cutoff is smaller than relevant *finite* scales in the theory, the distinction from single volume should be essentially unambiguous.

While the mechanism of vSChSB has not been satisfactorily clarified yet, one of the driving motivations for developing chiral polarization framework was to provide a possible indicator of the above type. It is important in that regard that, unlike $\rho(0)$, chiral polarization parameters Λ_{ch}, Ω_{ch} and Ω can be readily non-zero in finite volume. If forming chirally polarized layer around the surface of Dirac sea provides sufficient and necessary condition for producing vSChSB, as conjectures of the previous section propose, then chiral polarization characteristics represent viable candidates for such *finite-volume "order parameters"* indeed.

It is interesting that the situation in finite volume is in fact simpler than what we dealt with in the previous section. There are just three characteristics which, taking into account the convention on exact zeromodes, can only be non-zero simultaneously, effectively yielding a single finite-volume order parameter. Theory (M, T, V) is said to be in *chirally polarized phase* if chiral polarization characteristics are positive, say $\Omega(M, T, V) > 0$. We emphasize again that this provides a well-defined dynamical distinction between theories in finite volume based on their chiral behavior. However, in addition to this and the fact that $\Omega(M, T)$ is expected to be a valid order parameter in traditional sense, our notion of finite-volume order parameter for vSChSB involves another feature contained in the following statement consistent with available data.

Conjecture 3. *The following holds in every lattice-regularized* $(M, T) \in \mathcal{T}$ *at sufficiently large ultraviolet cutoffs* Λ_{lat}.

(I) *Chiral polarization characteristics exist and* $0 \leq \Lambda_{ch}(V) \ll \Lambda_{lat}$ *for sufficiently large* V.
(II) *The property of valence spontaneous chiral symmetry breaking is characterized by*

$$\Sigma > 0 \iff \Omega(V) > 0 \quad \text{for } V_0 < V < \infty \tag{25}$$

i.e. it occurs if and only if the theory is in chirally polarized phase in large finite volumes.
(III) $\rho_{ch}(\lambda, V)$ *is non-positive for* $\lambda > \Lambda_{ch}(V)$*, except possibly in the vicinity of* Λ_{lat}.

The conceptual novelty in the above statement is that the right-hand side of Eq. (25) does not involve explicit infinite volume limit. This is different e.g. from Conjecture 2″ wherein the infinite volume limit of $\Omega(M, T, V)$, while significantly easier to deal with than QMC, still has to be investigated: the theory could stay in chirally polarized phase for arbitrary large volumes, but with $\Omega(M, T, V)$ scaling to zero. However, Conjecture 3 proposes that it is impossible to approach chirally symmetric physics in infinite volume via finite-volume physics in chirally polarized phase.[8] In other words, it suggests that, at least sufficiently close to the continuum limit, vSChSB and dynamical chirality are inextricable.

[8] Note that, for discussion in paragraph preceding and motivating Conjecture 2″, this implies that options *(ii)* and *(iii)* don't occur.

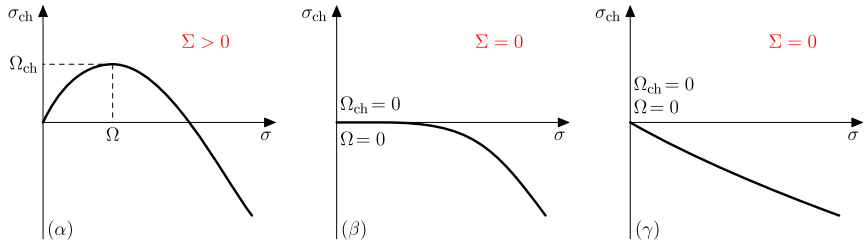

Fig. 3. Possible behaviors of $\sigma_{ch}(\sigma)$ in the vicinity of $\sigma = 0$. In finite volume, case (α) predicts vSChSB of infinite volume theory, while (β) and (γ) entail valence chiral symmetry.

We emphasize that the above is not to say that it is impossible to have a "finite volume correction" to prediction on vSChSB based on chiral polarization in single volume. However, in the realm of Conjecture 3, the false positive corresponds to missing out on the whole dynamically-defined phase. In other words, it is expected that only in very small volumes, when other aspects of physics are severely mutilated as well, is such occurrence likely.

Finally, we remark that while $\rho(\lambda = 0, V)$ and $\rho_{ch}(\lambda = 0, V)$ always vanish and cannot be utilized as indicators of vSChSB, this is not necessarily true for all strictly infrared constructs in finite volume. For example, in chirally broken case, $\lambda = 0$ is typically an isolated zero of $\rho(\lambda, V)$, but $C_A(\lambda = 0, V) \equiv \lim_{\lambda\to 0} \rho_{ch}(\lambda, V)/\rho(\lambda, V)$ is expected to be well-defined and positive. In fact, the strictly infrared version of Conjecture 3 with $\Omega(M, T, V)$ on the right-hand side of Eq. (25) replaced by $C_A(\lambda = 0, M, T, V)$ is an equally viable representation of the correspondence, albeit less appealing from practical standpoint.

2.5. σ-parametrization and the universal scale of vSChSB

For certain purposes, some of which are discussed below, it is useful to parametrize chiral polarization properties by cumulative eigenmode density σ, rather than Dirac spectral parameter λ. Recall that the description discussed so far is based on two cumulative densities, namely $\sigma(\lambda)$ and $\sigma_{ch}(\lambda)$: the behavior of $\sigma_{ch}(\lambda)$ defines polarization parameters Λ_{ch} and Ω_{ch}, while Ω emerges "a posteriori" from $\sigma(\lambda)$ and Λ_{ch}.

We wish to eliminate λ from the pair $\sigma(\lambda)$, $\sigma_{ch}(\lambda)$ and consider $\sigma_{ch} = \sigma_{ch}(\sigma)$. The latter is certainly a well-defined function when $\sigma(\lambda)$ is one-to-one, but this is also true in general case. Indeed, since $\sigma(\lambda)$ is non-decreasing and can have finite jumps, there are only two special circumstances to examine. (*a*) If $\sigma(\lambda)$ is constant on interval $[\lambda_1, \lambda_2]$ then multiple values of σ_{ch} could in principle be associated with $\sigma_1 = \sigma(\lambda_1)$. However, it follows from its definition that $\sigma_{ch}(\lambda)$ is then also constant on $[\lambda_1, \lambda_2]$, and $\sigma_{ch}(\sigma_1)$ is thus unique. (*b*) If $\sigma(\lambda)$ has a jump at $\bar{\lambda}$ with σ^l, σ^r being the left and right values respectively, then $\sigma_{ch}(\sigma)$ is a priori undefined on the interval (σ^l, σ^r). However, since the population of modes associated with interval (σ^l, σ^r) is assigned a common value of chiral correlation, namely $C_A(\bar{\lambda})$, there is a natural unique definition of $\sigma_{ch}(\sigma)$ on (σ^l, σ^r): the linear dependence whose graph connects the points $(\sigma^l, \sigma^l_{ch})$ and $(\sigma^r, \sigma^r_{ch})$. Here σ^l_{ch}, σ^r_{ch} are the left and right values of $\sigma_{ch}(\lambda)$ at $\bar{\lambda}$. Note that the slope of $\sigma_{ch}(\sigma)$ is $C_A(\sigma)$ for every σ.

There are few points we wish to emphasize regarding the utility of the above.

(i) Since $\sigma_{ch}(\lambda)$ can only have jumps at arguments where $\sigma(\lambda)$ does (see Appendix B), the function $\sigma_{ch}(\sigma)$ is not only well-defined but always continuous on its domain.[9] Given that $\sigma_{ch}(\sigma = 0) = 0$, there are then three possible behaviors of $\sigma_{ch}(\sigma)$ in the vicinity of zero: it can (α) turn positive, (β) remain identically zero or (γ) turn negative. While it simply classifies theories as chirally polarized, unpolarized or anti-polarized at lower spectral end, this dynamical distinction acquires deeper meaning in light of our conjectures. Indeed, in finite volume, the first case indicates that the theory is in chirally polarized phase, and is thus predicted to be chirally broken, as opposed to the remaining two options (see Fig. 3). In this way, the "low σ" behavior of $\sigma_{ch}(\sigma)$ provides for rather succinct and elegant representation of the ideas discussed here.

One noteworthy point in this regard is that when presented with $\sigma_{ch}(\sigma)$ in infinite volume only, the behavior (β) in itself is indefinite with regard to vSChSB. Indeed, it could correspond to the situation $\Omega_{ch} = 0$, $\Omega > 0$ with Ω undetermined by $\sigma_{ch}(\sigma)$ alone. In such case the information on large-volume behavior is needed to resolve the ambiguity.

(ii) In our discussion we paid little attention to the issues related to precise behavior of various new constructs in the continuum limit. In fact, this is not essential for our purposes. Indeed, our goal is to understand the dynamics of vSChSB, which means gaining insight in the regime of lattice theory where it becomes insensitive to the ultraviolet cutoff. Various "order parameters" we discussed are well-defined at arbitrary finite cutoff, and serve as indicators of vSChSB which itself is well-defined at arbitrary finite cutoff if chirally symmetric Dirac operator (overlap operator) is used.

Nevertheless, it is appealing to characterize chiral polarization via parameters with well-defined continuum values. As mentioned in [3] already, Λ_{ch} is expected to require a normalization factor to define its unique continuum limit e.g. in $N_f = 2 + 1$ zero temperature QCD at physical point.[10] However, the renormalization properties of mode density described in [10,11] imply that $\sigma_{ren}(\lambda_{ren}) = \sigma(\lambda)$ for renormalized/bare cumulative density. Hence, Ω is expected to be free of renormalization factors and have a universal continuum limit. The same would hold also for Ω_{ch} if the renormalization of $\rho(\lambda)$ and $\rho_{ch}(\lambda)$ proceeded via the same factor. This, however, would have to be established. Note that, in such case, the whole function $\sigma_{ch}(\sigma)$ would be universal.

(iii) Removing the reference to spectral parameter λ underscores the dynamical nature of the vSChSB $\leftrightarrow$ ChP equivalence. Indeed, in this form any explicit connection to "strictly infrared" scales, which has its roots in kinematic considerations, is eliminated. Rather, the correspondence relies exclusively on local dynamical behavior of lowest modes, irrespective of precise Dirac eigenvalues they are labeled with. Given that $\sigma_{ch}(\sigma)$ can be conveniently computed directly, without invoking the spectral representation, it is worthwhile to formulate the proposed connection directly in this language. In fact, the formulation becomes somewhat more concise: Ω is defined as the maximal $\bar{\sigma}$ such that $\sigma_{ch}(\sigma)$ is strictly increasing on $[0, \bar{\sigma}]$, while Ω_{ch} is always simply $\sigma_{ch}(\sigma = \Omega)$ due to continuity. The analog of Conjecture 3 is then as follows, with $\Omega(V)$ in Eq. (26) replaceable by $\Omega_{ch}(V)$ if so desired.

[9] In lattice units, this domain is in fact the interval [0, 12] since $N_c = 3$ for theories in $\mathcal{T}$. This is irrespective of volume, cutoff or lattice Dirac operator used.

[10] Note that in this discussion we implicitly assume that $D_{(1)} = D_{(2)} = D_{overlap}$ in Eq. (4), but we expect our points to apply whenever $D_{(2)} = D_{overlap}$.

Conjecture 3′. *The following holds in every lattice-regularized* $(M, T) \in \mathcal{T}$ *at sufficiently large ultraviolet cutoffs* Λ_{lat}.

(I) *Function* $\sigma_{ch}(\sigma, V)$ *is continuous on its domain* $\sigma \in [0, 12\Lambda_{lat}^4]$, *and* $\Omega(V) \ll 12\Lambda_{lat}^4$ *for sufficiently large* V.

(II) *The property of valence spontaneous chiral symmetry breaking is characterized by*

$$\Sigma > 0 \quad \Longleftrightarrow \quad \Omega(V) > 0 \quad \text{for } V_0 < V < \infty \tag{26}$$

(III) $\sigma_{ch}(\sigma, V)$ *is non-increasing for* $\sigma > \Omega(V)$, *except possibly in the vicinity of* $\sigma = 12\Lambda_{lat}^4$.

(iv) Relative to discussion in Ref. [3], our description of chiral polarization around the surface of Dirac sea became more detailed. In addition to the width of the polarized layer (Λ_{ch}), the phenomenon is also characterized by the volume density of total number of modes involved (Ω) and the associated total chirality (Ω_{ch}). In the spirit of Refs. [3,4] and the conjectures discussed here, we consider the corresponding scales, namely Λ_{ch}, $\Omega^{1/4}$ and $\Omega_{ch}^{1/4}$, to be the dynamical scales associated with the phenomenon of vSChSB. In the massless light-quark limit of "real-world QCD" (i.e. $N_f = 2 + 1$), they become the scales of SChSB. In Ref. [3] we estimated the (unrenormalized) value of chiral polarization scale in $N_f = 2+1$ QCD at physical point to be $\Lambda_{ch} \approx 80$ MeV. The estimated values of the other two parameters in this case are $\Omega^{1/4} \approx 150$ MeV (expected to be universal) and $\Omega_{ch}^{1/4} \approx 60$ MeV.

3. Temperature effects

In this section, we present results of the finite-temperature study in $N_f = 0$ QCD. This theory has a well-established deconfinement transition temperature T_c defined via expectation value of the Polyakov loop. According to the standard scenario, vSChSB disappears in close vicinity of T_c, but in general at some other temperature T_{ch}. We find that mode condensation and chiral polarization of valence overlap quarks exactly follow each other, in accordance with vSChSB–ChP correspondence. The data also shows that, at the fixed lattice cutoff used ($\Lambda_{lat} \simeq 2.3$ GeV), chiral transition temperature T_{ch} is strictly larger than T_c.

3.1. Lattice setup and Polyakov loop sectors

We simulate pure–glue SU(3) theory with Wilson action at $\beta = 6.054$. The non-perturbative parametrization of Ref. [15] is used to set the lattice scale, resulting in $a/r_0 = 0.170$ at the aforementioned gauge coupling. Using the standard value $r_0 = 0.5$ fm for reference scale, this translates into $a = 0.085$ fm. To perform a basic temperature scan, we vary the "time" extent of the lattice between $N_t = 4$ and $N_t = 20$ which corresponds to temperatures $T = 1/(N_t a)$ in the range 116–579 MeV. The spatial extent of the lattice is kept fixed at $N = 20$, corresponding to volume $V_3 = (Na)^3 = (1.7 \text{ fm})^3$. The information about these ensembles is summarized in Table 1 with some relevant explanations provided below.

Distinctive aspect of studying chiral issues in $N_f = 0$ theory relates to the fact that, while the deconfinement transition is associated with spontaneous breakdown of Z_3 symmetry signaled by the expectation value of Polyakov loop [16,17], Dirac spectral properties in the deconfined phase depend on which vacuum broken theory happens to visit. In particular, it was pointed out that valence chiral symmetry in the "real sector" might be restored at lower temperature than

Table 1
$20^3 \times N_t$ ensembles of $N_f = 0$ theory with Wilson gauge action ($\beta = 6.054$), used in the overlap eigenmode calculations. $|\lambda|^{av}_{\min}$ is the average magnitude of smallest non-zero eigenvalue in a configuration, while $|\lambda|^{av}_{\max}$ that of the largest one. The magnitudes of all computed non-zero eigenvalues in an ensemble satisfy $|\lambda|_{\min} \leq |\lambda| \leq |\lambda|_{\max}$.

Ensemble	N_t	T/T_c	T [MeV]	N_{cfg}	$\lvert\lambda\rvert^{av}_{\min}$	$\lvert\lambda\rvert_{\min}$	$\lvert\lambda\rvert^{av}_{\max}$	$\lvert\lambda\rvert_{\max}$
E_1	20	0.42	116	100	0.0204	0.0027	0.6128	0.6160
E_2	12	0.70	193	200	0.0320	0.0065	0.7241	0.7270
E_3	10	0.84	232	200	0.0379	0.0018	0.7658	0.7701
E_4	9	0.93	258	200	0.0402	0.0039	0.7912	0.7944
E_5	8	1.05	290	400	0.0859	0.0011	0.8208	0.8246
E_6	7	1.20	331	400	0.2473	0.0006	0.8631	0.8675
E_7	6	1.39	386	100	0.4038	0.0498	0.9233	0.9283
E_8	4	2.09	579	100	0.7868	0.7129	1.1608	1.1673

Table 2
$N^3 \times 7$ ensembles of $N_f = 0$ theory with Wilson gauge plaquette action ($\beta = 6.054$), used to study finite volume effects in the $N_t = 7$ system (E_6).

Ensemble	N	L [fm]	N_{cfg}	$\lvert\lambda\rvert^{av}_{\min}$	$\lvert\lambda\rvert_{\min}$	$\lvert\lambda\rvert^{av}_{\max}$	$\lvert\lambda\rvert_{\max}$
G_1	16	1.36	400	0.301513	0.005507	1.029540	1.034761
G_2	24	2.04	400	0.200300	0.000089	0.746919	0.753360
G_3	32	2.72	200	0.067461	0.000046	0.598446	0.607929

in the "complex sectors" [18], with the former transition being the one occurring close to T_c. While this conclusion remained somewhat controversial [19], it became common to study the real sector in connection with chiral symmetry restoration in $N_f = 0$ QCD. This is also tied to the fact that dynamical fermions tend to bias gauge fields correspondingly (see e.g. [20]), bringing up the expectation that the dynamics of the real-sector vacuum better resembles the behavior in real-world QCD.

Here we adopt the above point of view and present results for the real Polyakov loop sector. While in infinite volume the Z_3 distinction is only relevant above T_c, it is reasonable to keep the separation on both sides of the transition for finite system due to tunneling. To that effect, we rotated each generated configuration into complementary Z_3 sectors, but N_{cfg} of Table 1 refers to independent unrotated configurations. Except for ensembles E_1 and E_2, Dirac eigensystems were calculated in all Z_3 sectors for each configuration, and the statistics for real-phase results is thus N_{cfg}. For E_1 and E_2, only configurations originally generated in real sector, 31 and 61 of them respectively, were included. Overlap Dirac operator with Wilson kernel ($r = 1$) and $\rho = 26/19$ was used in these valence quark calculations, and the quoted spectral bounds refer to the real Polyakov-loop sector. For all ensembles used in this work, 200 lowest eigenmodes with non-negative imaginary part were computed.

We use $T_c/\sqrt{\sigma} = 0.631$, quoted in Ref. [21], as a reference value for infinite-volume continuum-limit transition temperature to label our ensembles. With string tension value $\sigma = (440\ \text{MeV})^2$ this translates into $T_c = 277$ MeV. Since the volume and lattice cutoff are finite, and there is also a small uncertainty in the determination of the lattice scale, it is prudent to check whether Z_3 transition in our system occurs in the expected range of temperatures. To do so, we show the scatter plot of the Polyakov loop in Fig. 4(left). As can be seen quite clearly, the expected symmetric distribution below T_c is contrasted with Z_3-concentrated population above T_c. This is also confirmed by the behavior of Polyakov-loop susceptibility shown in Fig. 4(right).

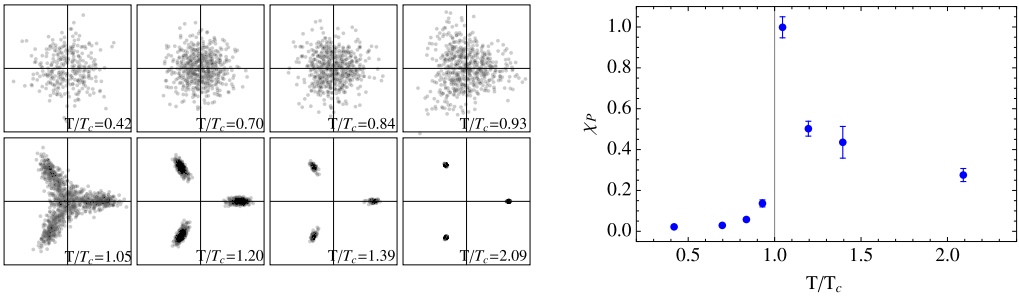

Fig. 4. Left: scatter plots of Polyakov loop for ensembles E_1–E_8. Each point corresponds to a configuration with Z_3 symmetrization included. Sliding scale has been adjusted in each case so as to contain all points. Right: Polyakov-loop susceptibilities.

There is thus little doubt that ensembles E_1–E_4 and E_5–E_8 represent the system in confined and deconfined phases respectively.

In the course of our analysis it will turn out that, while clearly in the deconfined phase, the $N_t = 7$ system still exhibits chiral polarization and vital signs of vSChSB. To ascertain this, we study the finite-volume behavior on additional lattices with details given in Table 2. The ensemble G_3 with $V_3 = (2.72\ \text{fm})^3$ corresponds to the largest system studied. All the above notes concerning E-ensembles also apply to G-ensembles.

3.2. Raw data

One useful way to obtain a quick overview of the situation at hand is to examine the scatter plots of C_A versus λ since they provide a simultaneous qualitative picture of spectral abundance and chiral polarization. Thus, each eigenmode associated with given ensemble contributes a point to the plot, specified by the magnitude of the eigenvalue (λ) and its correlation coefficient of polarization (C_A). In Fig. 5 we show these plots for E-ensembles. Note that the temperature increases in lexicographic order.

Regarding the vSChSB $\leftrightarrow$ ChP correspondence, the main aspect to examine is whether presence of near-zeromodes is always associated with tendency for chiral polarization at low energy, and that chiral polarization is always absent in accessible spectrum if near-zeromodes are not produced. Such qualitative correlation is clearly observed in Fig. 5.

Quick look at scatter plots also suggests three kinds of qualitative behavior as the temperature is increased. First, the "low-temperature dynamics", exemplified by E_1 ($T/T_c = 0.42$) and discussed extensively in [3], appears to apply throughout the confined phase. Second, the "transition dynamics", exemplified by E_6 ($T/T_c = 1.20$) extends approximately from T_c to chiral transition point T_{ch}. It is characterized by the spectral separation of near-zeromodes from the bulk and the creation of mode-depleted region between them. Finally, the "high-temperature dynamics" turns on above T_{ch} as near-zeromodes can no longer be supported in sufficient numbers, and the anti-polarization of the bulk takes over.

In the above temperature scan, the system associated with ensemble E_6 ($T/T_c = 1.20$) is of prime interest: not only does it suggest itself as a lattice example of vSChSB with deconfined gauge fields [14] but, more importantly, it is the most borderline case where the vSChSB $\leftrightarrow$ ChP association should be ascertained. To do this at the level of raw data, we show in Fig. 6 the λ–C_A scatter plots for this system in increasing 3-volumes. The abundance of near-zeromodes clearly rises with volume, with the layer of high concentration increasingly focused toward the

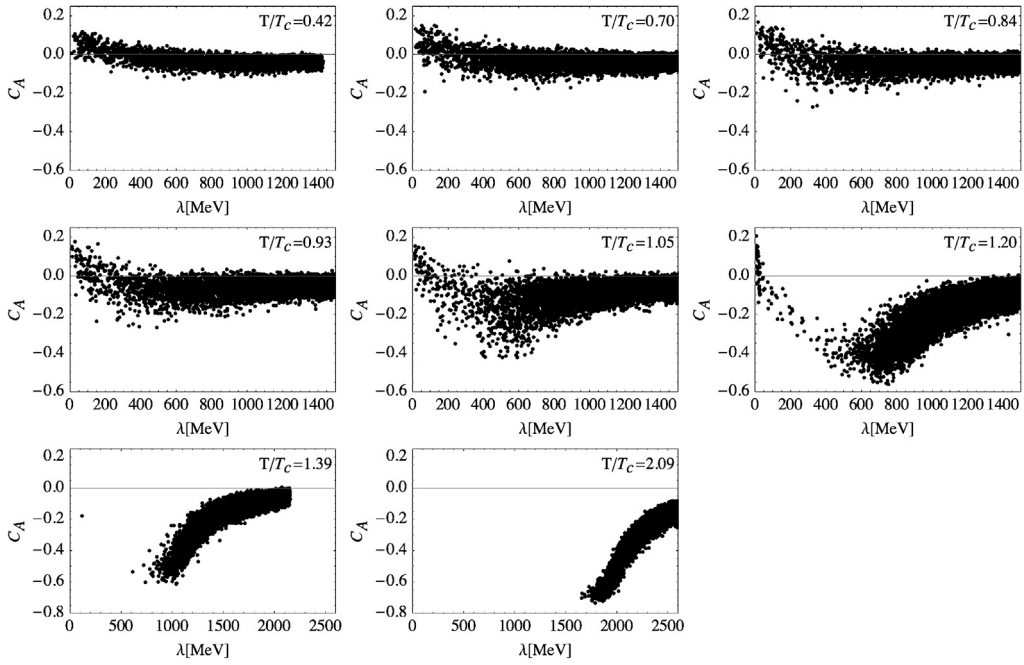

Fig. 5. Scatter plots of chiral polarization correlation (C_A) versus eigenvalue magnitude (λ) for E-ensembles of Table 1. Note the change of scale for E_7, E_8 relative to E_1–E_6.

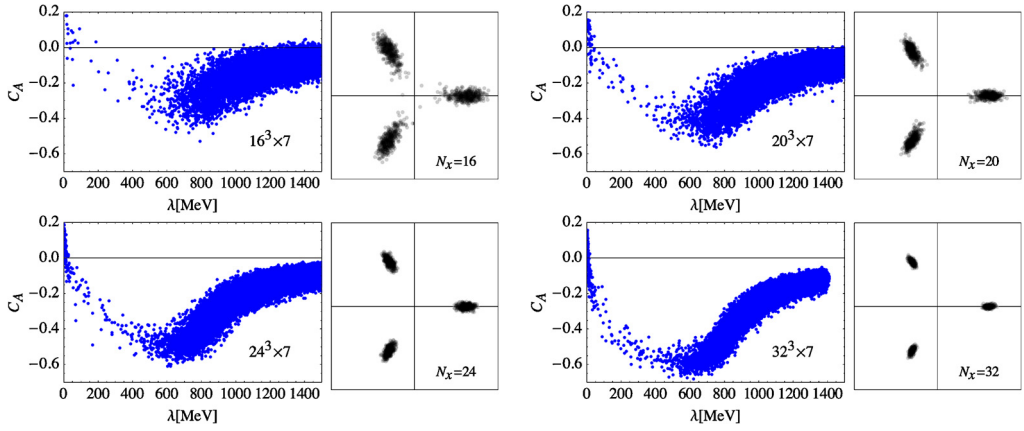

Fig. 6. Scatter plots (C_A vs. λ) for $N_t = 7$ system ($T/T_c = 1.20$) in varying spatial volume. The associated raw data for Polyakov loop is also shown.

origin. Thus, mode condensation appears all but inevitable. At the same time, chiral polarization persists as predicted. Decreasing width of the polarized layer suggests possible singular behavior in the vein of our discussion in Section 2.3. Note that we also show the associated scatter plots of Polyakov loop, clearing any suspicion that the system could be in confined phase.

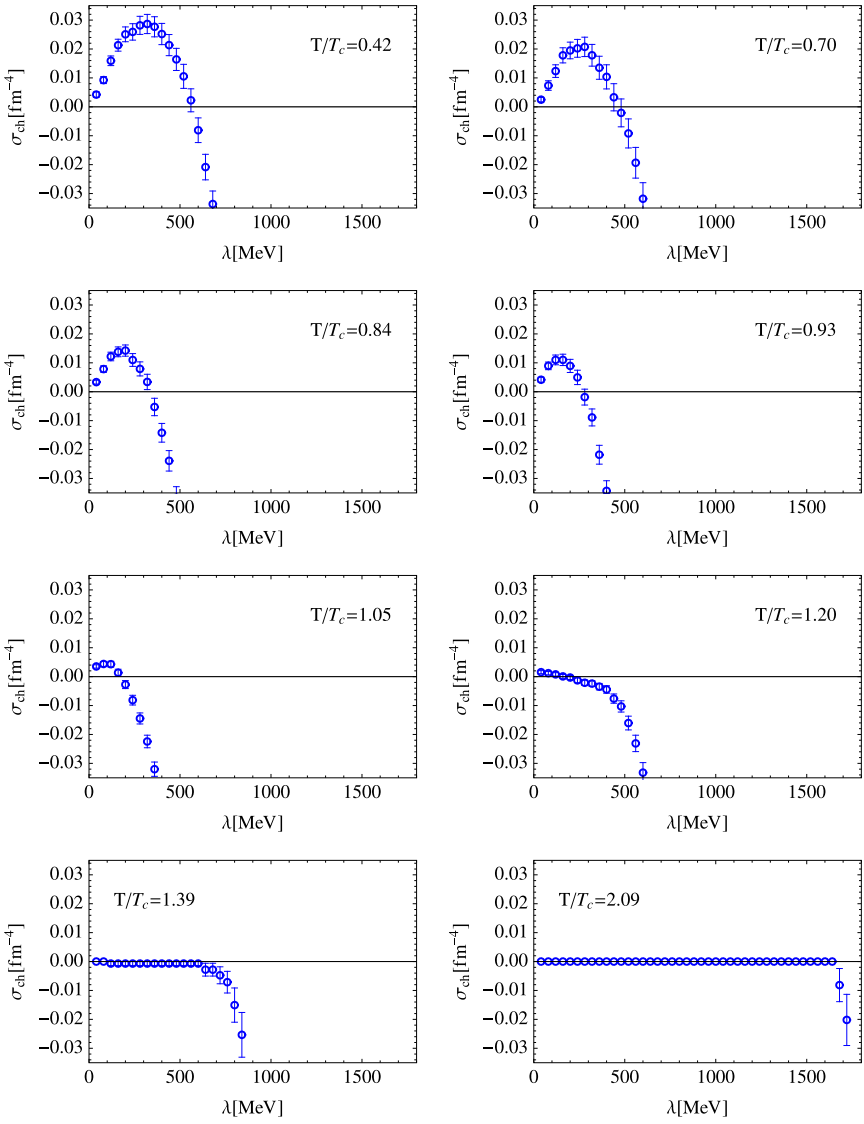

Fig. 7. Cumulative chiral polarization density for all E-ensembles. Ranges are fixed.

3.3. *Chiral polarization transition*

We now start putting the observations of the previous section into more formal terms. The first task in this process is to determine the transition point (in temperature) for chiral polarization. It should be emphasized that whether the system is in the polarized phase or not is a well-defined question in any finite volume. The temperature scan will be performed for E-ensembles sharing the same 3-volume. Resulting transition point is thus associated with the corresponding ultraviolet cutoff and volume.

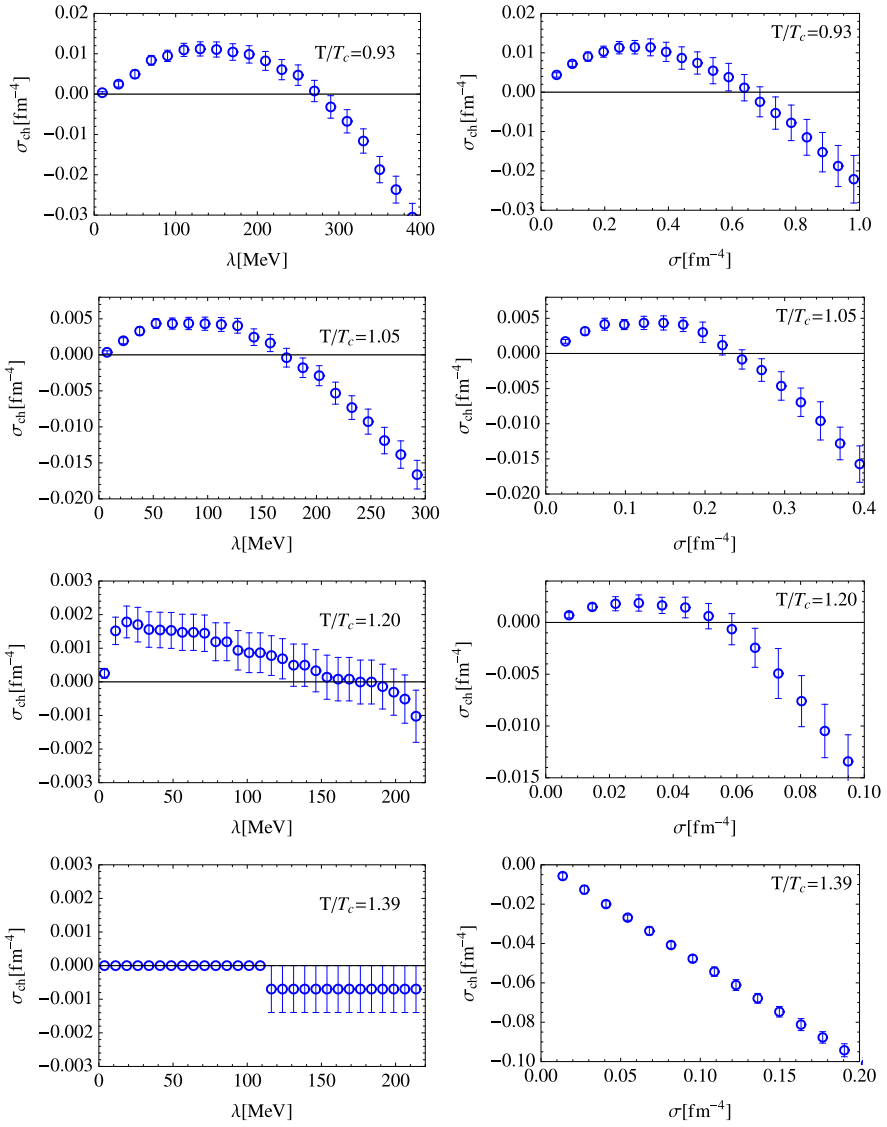

Fig. 8. Low-energy closeup of $\sigma_{ch}(\lambda)$ (left column) and $\sigma_{ch}(\sigma)$ (right column) for ensembles E_4–E_7. Theory is clearly chirally polarized at $T/T_c = 1.20$. Note the sharp transition in the latter representation when changing to $T/T_c = 1.39$.

To do this in a straightforward way, we monitor the behavior of cumulative chiral polarization density $\sigma_{ch}(\lambda)$. The result is shown in Fig. 7 with temperature increasing in lexicographic order. The characteristic positive bump (see discussion for Fig. 2) appears at low temperatures signaling the creation of chirally polarized layer around the surface of the Dirac sea. Data is shown on identical scales for all ensembles to see the changing position of the maximum (Λ_{ch}) as well as its value (Ω_{ch}). The polarization feature is clearly absent at $T/T_c = 1.39$, while it appears to be present at the borderline case ($T/T_c = 1.20$) which, however would benefit from better resolution.

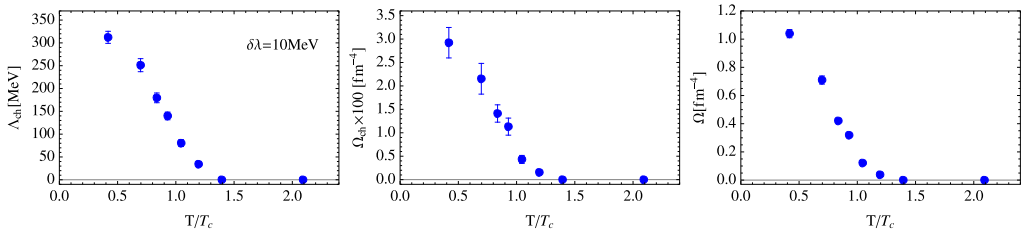

Fig. 9. Global characteristics of chiral polarization in E-ensembles as functions of temperature. They indicate the transition temperature $1.2T_c < T_{ch} < 1.39T_c$ for the cutoff and volume in question. $\delta\lambda$ refers to coarse-graining parameter used in determination of Λ_{ch}.

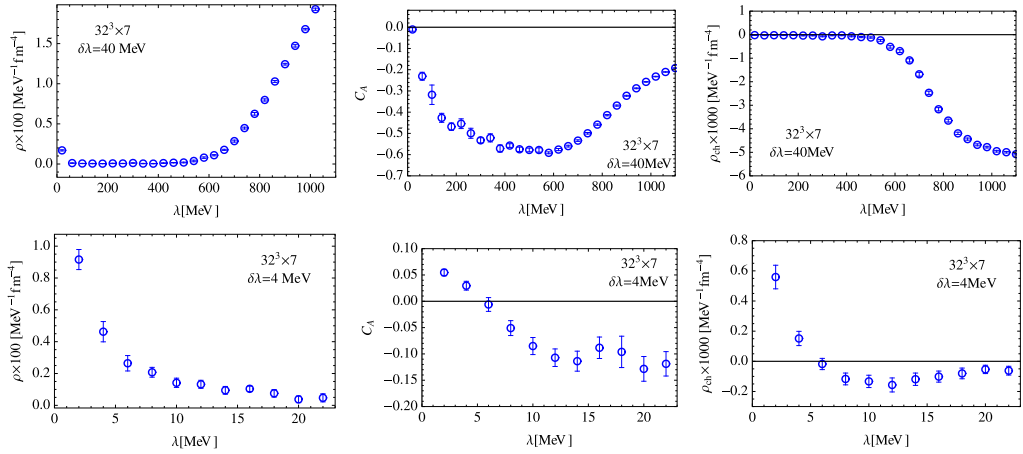

Fig. 10. Large view (top) and closeup (bottom) of $\rho(\lambda)$, $C_A(\lambda)$, $\rho_{ch}(\lambda)$ for ensemble G_3.

In Fig. 8 we show closeups of the low part of the spectrum for ensembles E_4–E_7. Note that the scales are no longer fixed in order to properly resolve the polarization feature. Temperature grows from top to bottom with left column displaying $\sigma_{ch}(\lambda)$ and the right column the associated $\sigma_{ch}(\sigma)$. As advertised, and suggested by the raw data, at $T/T_c = 1.20$ the system is still in chirally polarized phase. Both $\sigma_{ch}(\lambda)$ and $\sigma_{ch}(\sigma)$ tell the same story, but note how the latter effectively removes the depleted regions of the Dirac spectrum (ensembles E_6 and E_7) from consideration, focusing on polarization properties of existing modes.

Finally, in Fig. 9 we show the temperature dependence for the three global characteristics of the chirally polarized layer, namely Λ_{ch}, Ω_{ch} and Ω. As discussed in Section 2.4, they are all equivalent indicators of chiral polarization in finite volume, and potentially *finite-volume order parameters* of vSChSB, as proposed by Conjecture 3.

3.4. *Infinite volume*

To test the proposed conjectures, it is necessary to deal with infinite volume considerations since the definition of vSChSB explicitly relies on it. In more concrete terms, it is important to check which forms of Conjecture 2 (if any) apply to the finite-cutoff situation at hand. Also, assessing possible merits in the notion of finite-volume order parameter, associated with Conjecture 3, depends on the behavior of polarization observables in large volumes.

As is clear from our discussion in preceding sections, the relevant situation to study in this regard is $T/T_c = 1.2$, represented by E_6 and the G-ensembles. Indeed, this is the borderline case, providing the most sensitive test for vSChSB–ChP correspondence. To overview the situation directly in the largest volume available ($N = 32$), we show in Fig. 10(top) the triplet of characteristics $\rho(\lambda)$, $C_A(\lambda)$, $\rho_{ch}(\lambda)$ over a large spectral range, fully covering the depleted region observed in the raw data. While the increased density near the origin is clearly visible, chiral polarization feature is not recognizable at this resolution. However, closeup to the vicinity of the origin in Fig. 10(bottom) reveals a clear polarized layer as anticipated. Note that the feature became quite thin in this largest volume.

To examine the situation in detail, we first focus on the ChP side of the correspondence. In practical terms, this means determining the form of the chiral polarization layer for large and infinite volume. To that effect, we show in Fig. 11 the behavior of $\sigma_{ch}(\sigma)$ for the four volumes available. As pointed out in the previous section, this is the most robust way of visualizing the layer in case of depleted spectra such as those we are dealing with in the transition region. Indeed, even though Fig. 6 indicates severe depletion (even close to the spectral origin) for the $N = 16$ system, the polarization layer is still quite clearly visible in $\sigma_{ch}(\sigma)$. In larger volumes, the characteristic positive bump tends to grow both in σ and σ_{ch}-directions, strongly suggesting that the ChP layer remains the dynamical feature of the system in the infinite volume limit.

There is, however, a difference in how infinite-volume ChP is realized at $T/T_c = 1.2$ and at zero or small temperatures. This is revealed in Fig. 12 where we show the dependence of chiral polarization parameters on the infrared cutoff. As foretold by Fig. 11, Ω_{ch} and Ω grow as the cutoff is removed, but Λ_{ch} decreases, likely toward zero. Continuation of these trends in larger volumes is only possible when $\rho(\lambda, V)$ and $\rho_{ch}(\lambda, V)$ develop a $\delta(\lambda)$-core in $V \to \infty$ limit, to keep the observed volume density of polarized modes and volume density of dynamical chirality finite. We may thus be dealing with a singular case of the type ($\Lambda_{ch} = 0$, $\Omega_{ch} > 0$, $\Omega > 0$) discussed repeatedly in Section 2. Including such ChP behaviors was the main motivation behind extending our formalism to current form.

Let's now examine the vSChSB side of the correspondence. This might seem unnecessary from strictly logical standpoint since the result of our ChP analysis is such that it already carries with it the implication of vSChSB (with divergent condensate) at $T/T_c = 1.2$. However, it certainly helps the case if the same conclusion can also be reached on its own, independently of chiral polarization. We thus wish to check directly whether dynamics at $T/T_c = 1.2$ is consistent with the definition of mode-condensing theory. To begin with, note that the behavior of $\rho(\lambda)$ for largest volume available, shown in the lower-left plot of Fig. 10, is in itself strongly suggestive of mode condensation. Indeed, contrary to monotonically increasing function typical of zero and low temperatures, this $\rho(\lambda)$ is monotonically decreasing in the very infrared range shown. One thus naively expects non-zeromode density to survive at the spectral origin.

However, the definition (10) of mode condensation demands that volume trends be examined at fixed infrared spectral windows to make meaningful conclusions. In line with this definition, we consider the coarse-grained version of $\rho(0)$, namely

$$\rho(\lambda = 0, \Delta, V) \equiv \frac{1}{\Delta}\sigma(\lambda = \Delta, V) \tag{27}$$

to see the associated volume tendencies for various values of Δ. The result of such calculation for a range of infrared windows down to 4 MeV is shown in Fig. 13. Note that for any fixed V, function $\rho(0, \Delta, V)$ will approach zero for $\Delta \to 0$. This is explicitly seen in $N = 16$ and 20 cases but not for the two larger 3-volumes where the downward bend occurs at yet smaller

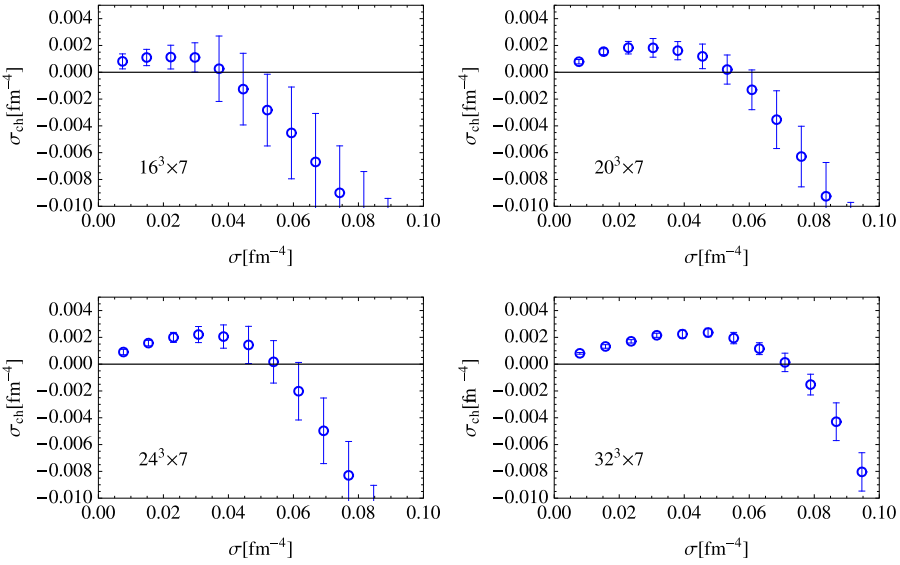

Fig. 11. Polarization characteristic $\sigma_{ch}(\sigma)$ at $T/T_c = 1.2$ for increasing 3-volumes.

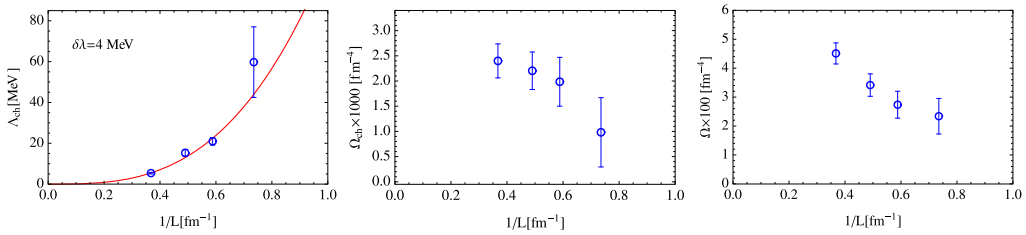

Fig. 12. Global characteristics of chiral polarization at $T/T_c = 1.2$ against infrared cutoff. Simple power-law fit was included in case of $\Lambda_{ch}(1/L)$ to guide the eye.

values of Δ. Important feature of these results is that $\rho(0, \Delta, V)$ grows with volume for all Δ shown. In fact, the rate of growth increases at small Δ, and even before the occurrence of the bend, leaving little room for the possibility that $\lim_{\Delta\to0}\lim_{V\to\infty}\rho(0, \Delta, V)$ vanishes. Rather, the data is consistent with diverging mode condensate as expected from ChP analysis.

To summarize, we presented evidence that the layer of chirally polarized modes around the surface of the Dirac sea remains the feature of $N_f = 0$ QCD at $T/T_c = 1.2$ even in the infinite-volume limit. At the same time, the system was found to be mode-condensing, in accordance with the general vSChSB–ChP correspondence. The specific form of ChP layer conforms to the types described by Conjectures 2′, 2″, but most likely doesn't fall into the realm of Conjecture 2. We emphasize that this doesn't mean that Conjecture 2 is invalid: this would only transpire if the concluded type of ChP behavior persisted at arbitrarily large ultraviolet cutoff. Note also that our analysis is in agreement with Conjectures 3, 3′, thus lending support to the concept of finite-volume order parameter.

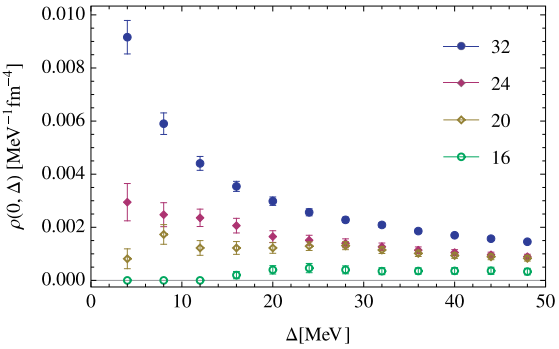

Fig. 13. Coarse-grained mode condensate $\rho(0, \Delta)$ at $T/T_c = 1.2$ for increasing 3-volumes.

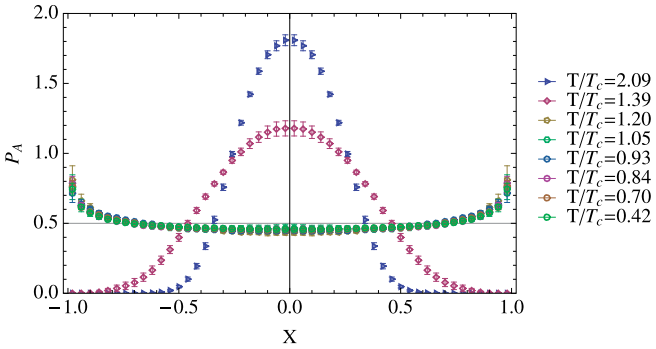

Fig. 14. The absolute X-distribution $P_A(X, \sigma \to 0)$, i.e. for lowest modes in E-ensembles.

3.5. Absolute X-distributions at finite temperature

In the previous analysis of QCD phase transition, we focused on spectral properties based on the correlation coefficient of chiral polarization C_A. Indeed, this is sufficient for formulating and verifying the vSChSB–ChP correspondence which is our main focus here. However, for other purposes involving vacuum structure, more detailed information contained in absolute X-distributions $P_A(X)$ might be valuable. In Ref. [4] (Proposition 1) it was concluded that, in $N_f = 0$ QCD at zero temperature, $P_A(X)$ has a simple behavior for low-energy Dirac eigenmodes: it is either purely convex or purely concave, with the former being associated with polarization while the latter with anti-polarization. It is thus a natural question to ask whether something different happens in this regard due to thermal agitation.

To start such inquiry, we wish to establish how X-distribution of lowest modes changes with temperature and, in particular, whether a qualitative shift occurs when crossing the chiral transition point T_{ch}. To formalize this question, it is preferable to think in terms of $P_A(X, \sigma)$ rather than the canonical $P_A(X, \lambda)$ of Eq. (17). Indeed, this puts the low-temperature systems with abundance of small eigenvalues, and the high-temperature systems with low-energy depletion, on the same footing. We are then interested in $P_A(X, \sigma \to 0)$ which in practice needs to be coarse-grained with respect to σ. The latter is accomplished by considering $P_A(X, \sigma = 0, \Delta)$, which represents $P_A(X, \sigma)$ averaged over $\sigma \in [0, \Delta]$.

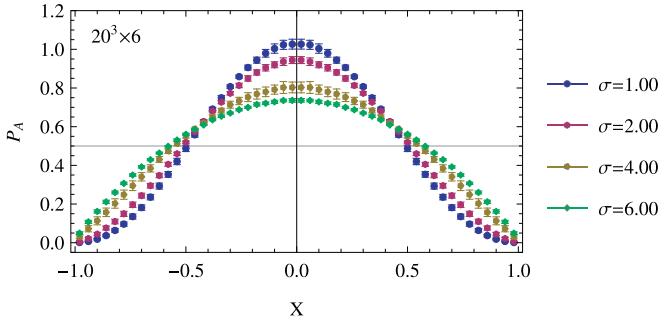

Fig. 15. The absolute X-distribution $P_A(X, \sigma, \delta = 0.2)$ for ensemble E_7 $(T/T_c = 1.39)$ with increasing values of σ. Value $\delta = 0.2$ entails averaging over 46 eigenmodes.

The result of such calculation for E-ensembles is shown in Fig. 14. We chose to fix the (total) number of included modes to 25 for each system, which corresponds to small coarse-graining parameter Δ in the range 0.02–0.15 fm^{-4}. This statistics is also sufficient to verify that further lowering this cut doesn't change the behavior of absolute X-distribution. As one can see, chiral transition is dramatically reflected in $P_A(X, \sigma = 0)$: we observe a new type of functional behavior above T_{ch} (ensembles E_7 and E_8), namely that of indefinite convexity. To specify the convexity properties more precisely, we will implicitly view $P_A(X)$ as defined on a positive chiral branch, namely $X \in [0, 1]$, in what follows. The new behaviors we found are then characterized by presence of a single inflection point $X_0 \in (0, 1)$ of the type concave-to-convex, i.e. $P_A(X)$ is concave on $[0, X_0]$ and convex on $[X_0, 1]$.

Conjecture 4. *Consider lattice-regularized $N_f = 0$ theory at arbitrary temperature T. Let $T_{ch} = T_{ch}(\Lambda_{lat}, V_3)$ be the temperature of chiral polarization transition at sufficiently large ultraviolet cutoff Λ_{lat}, and sufficiently large 3-volume V_3. Then absolute X-distribution $P_A(X, \sigma = 0)$ is convex for $T < T_{ch}$, and has a single inflection point of type concave-to-convex for $T > T_{ch}$.*

Note that in the fixed-scale approach, utilized in our numerical work, the set of accessible temperatures is discrete. Thus, rather than a unique T_{ch} at fixed finite Λ_{lat}, there is a range associated with the two successive values of N_t across which the transition occurs. This is implicitly understood in the above. A fine-grained question in this regard is whether there could be a brief phase above T_{ch} where $P_A(X, \sigma = 0)$ is concave, and which cannot be resolved at the lattice cutoff we are using.

The above finding naturally raises questions about the prevalence of modes with indefinite convexity in the bulk of the finite-temperature spectrum. First of all, we have not found any modes of indefinite convexity for $T < T_c$. The absence of such modes at zero temperature was the main part of Propositions 1, 3 in Ref. [4], and it carries over to this wider regime. The proposed statement in the language used here is as follows.

Conjecture 5a. *Consider lattice-regularized $N_f = 0$ theory at temperature $T < T_c = T_c(\Lambda_{lat})$. If $\Omega = \Omega(\Lambda_{lat}, V_3)$ is the density of chirally polarized modes, then the following holds at sufficiently large Λ_{lat} and V_3. Absolute X-distribution $P_A(X, \sigma)$ is (i) convex in X for $\sigma \in (0, \Omega)$, (ii) uniform for $\sigma = \Omega$, and (iii) concave at least for some band $\sigma > \Omega$.*

It turns out that the situation is in fact analogous for $T > T_{ch}$ except that the role of chirally polarized (convex) modes is assumed by modes with indefinite convexity of $P_A(X)$. To support this, we show in Fig. 15 the sequence of absolute X-distributions with increasing σ for ensemble E_7. Note that for non-zero values of σ we use symmetric coarse-graining, averaging over the interval $(\sigma - \delta/2, \sigma + \delta/2)$. The data suggests the existence of a point $\sigma = \Omega_1$ where the behavior changes from convex-indefinite to concave. At this particular temperature the transition occurs in the vicinity of $\Omega_1 \approx 3.0\ \text{fm}^{-4}$ and a precise determination can be performed if desired. We are thus led to formulate the following statement.

Conjecture 5b. *Consider lattice-regularized $N_f = 0$ theory at temperature $T > T_{ch} = T_{ch}(\Lambda_{lat}, V_3)$. At sufficiently large Λ_{lat} and V_3 there exists $\Omega_1 = \Omega_1(\Lambda_{lat}, V_3, T)$ such that the following holds. Absolute X-distribution $P_A(X, \sigma)$ (i) has a single inflection point of type concave-to-convex for $0 < \sigma < \Omega_1$ and (ii) is concave at least for some band $\sigma > \Omega_1$.*

We finally turn to the "mixed phase" ($T_c < T < T_{ch}$). This dynamics exhibits chiral polarization ($\Omega > 0$), which in case of confined vacuum happens to be synonymous with convexity of $P_A(X)$ for $\sigma < \Omega$. However, Conjecture 5b suggests that deconfinement is tied to indefinite convexity of absolute X-distributions. How then is the coexistence of vSChSB and deconfinement, and thus of chiral polarization and indefinite convexity, realized in the mixed phase? The specific arrangement we found is exemplified via ensemble G_3 in Fig. 16. The spectrum starts with a layer of convex modes (top left), like at low temperatures, but the distribution loses its definite convexity for $\Omega' < \sigma < \Omega_1$, after which it becomes concave (bottom right). There is a band $\Omega_0 < \sigma < \Omega_1$ within the convex-indefinite regime, where modes are of the type found at $T > T_{ch}$, i.e. their $P_A(X)$ has one concave-to-convex inflection point (bottom left). We thus propose the following.

Conjecture 5c. *Consider lattice-regularized $N_f = 0$ theory at finite temperature and overlap valence quarks. There exist lattice cutoffs Λ_{lat} such that $T_c(\Lambda_{lat}) < T_{ch}(\Lambda_{lat}, V_3)$ for sufficiently large V_3. At temperatures $T_c < T < T_{ch}$ there are $\Omega' < \Omega_0 < \Omega_1$ such that $P_A(X, \sigma)$ is (i) convex for $0 < \sigma < \Omega'$, (ii) convex-indefinite but not of type (iii) for $\Omega' < \sigma < \Omega_0$, (iii) has one inflection point of concave-to-convex type for $\Omega_0 < \sigma < \Omega_1$, and (iv) is concave at least for some band $\sigma > \Omega_1$. Moreover, $\Omega' < \Omega < \Omega_0$.*

It should be pointed out that the convex-indefinite spectral band of *(ii)* may just be the "reversed" version of *(iii)*, namely that the associated $P_A(X)$ has a single inflection point of convex-to-concave type. However, our statistics is not large enough to support this aspect with sufficient certainty. Note also that the above formulation doesn't explicitly exclude the possibility that $\Omega' = 0$, neither in finite volume nor in the infinite volume limit.[11] However, Ω_0 is predicted to be positive in both cases since Ω is.

3.6. Dirac mode landscape at finite temperature

According to vSChSB–ChP correspondence, chiral symmetry restoration at finite temperature is the process of chiral depolarization (positive C_A becoming negative) in the Dirac spectrum.

[11] This doesn't necessarily contradict Conjecture 4 which is only concerned with the limit $P_A(X, \sigma \to 0)$.

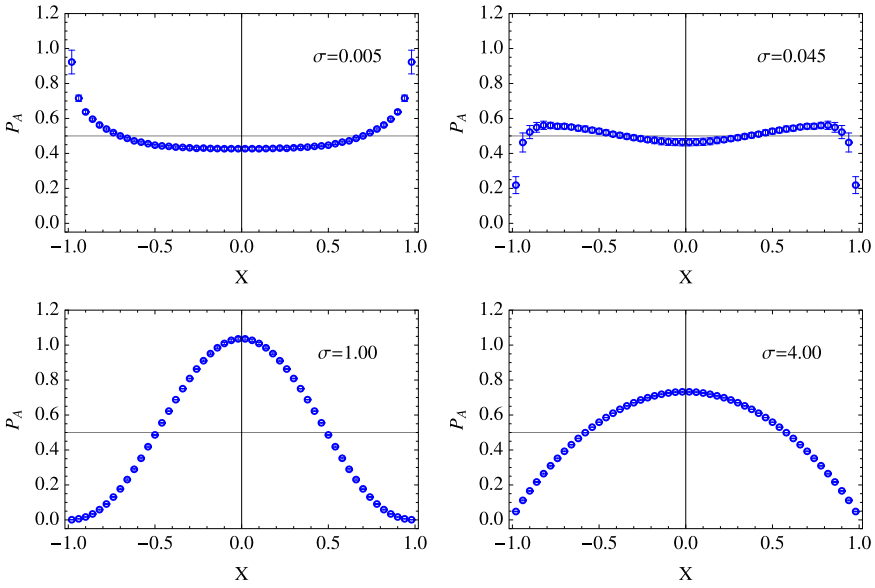

Fig. 16. Absolute X-distributions in ensemble G_3 for increasing σ representing four kinds of behavior found. The upper two results were obtained with coarse-graining parameter $\delta = 0.01$ (23 modes), while $\delta = 0.2$ (460 modes) was used for the lower two.

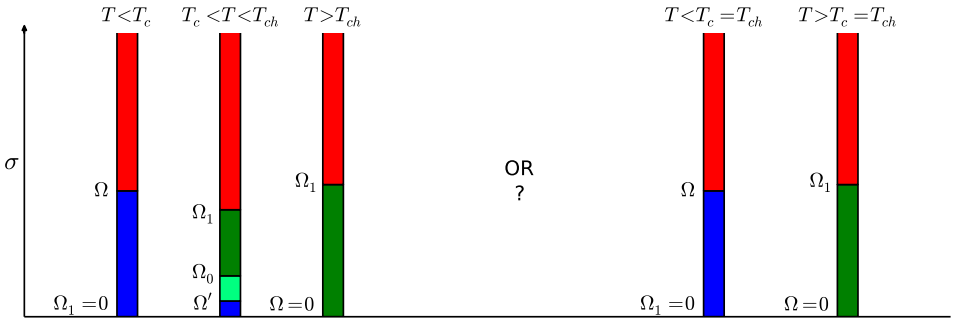

Fig. 17. Schematic view of Dirac eigenmodes at finite temperature according to their absolute X-distributions with blue representing convexity, red concavity, and shades of green indefinite convexity. The left side corresponds to continuum-limit scenario with $T_c < T_{ch}$ when the mixed phase (middle bar) exists, while the right side to scenario with $T_c = T_{ch}$.

However, results of the previous section suggest that more detailed polarization characteristic – absolute X-distribution – encodes *both* major effects of thermal agitation: valence chiral symmetry restoration and deconfinement. This information is stored in convexity properties of $P_A(X)$ which can in this case even be invoked on their own, without explicit reference to C_A. The resulting eigenmode "convexity landscape" is schematically shown in Fig. 17 with blue and red color marking purely convex and purely concave behavior of $P_A(X)$ respectively. The two shades of green represent convex-indefinite $P_A(X)$, with darker version signifying the presence of a single concave-to-convex inflection point.

Notice that Fig. 17 offers two scenarios for possible behavior in the vicinity of QCD phase transition. Indeed, whether *continuum* $N_f = 0$ QCD exhibits the mixed phase or not remains an

open issue, and the formulation of Conjecture 5c reflects this status. Thus, the option with mixed phase is shown on the left, and the one without it on the right. Regardless of which possibility is realized in the continuum however, the results provide for definite and somewhat unexpected new characterization of confinement via chirality properties.

In $N_f = 0$ QCD at finite temperature, confined vacuum supports $P_A(X)$ of definite convexity in overlap Dirac modes, while deconfined vacuum produces a band of modes with convex-indefinite $P_A(X)$ at low σ.

With regard to the situation at high temperature ($T > T_{ch}$), one should mention a possible connection of these findings to recent works, proposing that QCD phase transition can be viewed as a version of Anderson localization, with increasing temperature controlling the degree of randomness [22–24]. In this scenario, there is an analogue of Anderson's mobility edge, below which Dirac modes are localized. Given that absolute X-distribution is a fully dynamical characteristic of the modes, it is reasonable to put forward the hypothesis that the suggested mobility edge is associated with "concavity edge" Ω_1 from the above analysis. Denoting by $\lambda = \Lambda_{ch1}$ the spectral scale corresponding to Ω_1, it is natural to expect that the mobility edge in fact coincides with Λ_{ch1}. The merits of this hypothesis need to be examined in a detailed dedicated study.

4. Effects of many light flavors

The second and qualitatively different route toward chiral symmetry restoration within $\mathcal{T}$ proceeds via including increasing number of dynamical quark flavors. While the general tendency is significantly more general, the usual setup deals with N_f massless flavors at zero temperature. Owing to numerous lattice studies, as well as other considerations, there is very little doubt that the canonical $N_f = 2$ case exhibits SChSB. However, massless fermions weaken the running of the gauge coupling, and it is expected that there is a critical number of flavors $N_{f,cr}$, beyond which chiral symmetry remains unbroken. The existence of $N_{f,cr}$ is connected to a larger issue, namely the existence of a "conformal window" in flavor, containing theories with infrared fixed point [25]. Indeed, this is expected to occur at $N_{f,cr} < N_f < 16.5$ for SU(3), and the reliable determination of $N_{f,cr}$ is of an ongoing interest. The specific issue whether $N_f = 12$ theory belongs to the conformal window gained a particular attention recently, as discussed e.g. in reviews [26–28].

Rather than entering the discussion of unresolved problems such as the above, our aim is to check the plausibility of vSChSB–ChP correspondence in this important corner of quark–gluon dynamics. It should be kept in mind that the validity of the proposed relation is to be examined for any given lattice regularization of any given theory from $\mathcal{T}$: it either holds or not for the regularized system at hand. We will thus not be much concerned with extrapolating quark mass to zero, or detailed issues of continuum limit. Instead, our goal is to check the correspondence in the situation where the effect of many light fermions is apparent, and the possibility for valence chiral restoration exists.

4.1. Lattice setup

For purposes of this pilot inquiry, we obtained some of the previously generated $N_f = 12$ staggered fermion ensembles described in Ref. [29]. More specifically, the regularization in question uses a negative adjoint plaquette term (coupling β_A) in addition to fundamental plaquette (coupling β_F), and nHYP-smeared staggered fermions. This arrangement helps with ameliorating the

Table 3
Ensembles of $N_f = 12$ lattice QCD with nHYP smeared staggered fermions and fundamental-adjoint (β_F–β_A) gauge plaquette action [29].

Ensemble	Size	β_F	β_A/β_F	am	N_{conf}	$\lvert\lambda\rvert^{av}_{\min}$	$\lvert\lambda\rvert_{\min}$	$\lvert\lambda\rvert^{av}_{\max}$	$\lvert\lambda\rvert_{\max}$
S_1	$16^3 \times 32$	2.8	−0.25	0.0200	100	0.0098	0.0007	0.5190	0.5259
S_2	$32^3 \times 64$	2.8	−0.25	0.0025	30	0.0007	0.0001	0.2016	0.2035
S_3	$24^3 \times 48$	2.8	−0.25	0.0025	50	0.0193	0.0001	0.3046	0.3075

problems of spurious UV fixed points and the unphysical lattice phases encountered in theories with many light flavors. Such issues have been carefully studied in this particular setting [30], and are not expected to arise for ensembles listed in Table 3.

Simulations of many-light-flavor systems have to deal with the fact that the equilibrium gauge fields are quite rough at currently accessible lattice cutoffs. Incorporating smearing into definition of lattice Dirac operator helps to make such calculations feasible. To define our overlap chiral probe, we use the same smearing procedure that was used in Monte Carlo generation of the ensembles. Nevertheless, it is prudent to exercise some care when using overlap operator even on fields that are moderately rough. Indeed, the physical branch of the Wilson–Dirac spectrum can shift significantly away from the origin on such backgrounds, and the mass parameter $\rho \in (0, 2)$ in overlap construction needs to be chosen sufficiently large to contain it. To avoid potential issues of this kind, we set $\rho = 1.55$, which is somewhat larger than $\rho = 26/19 \approx 1.37$ used in our "real world QCD" simulations. Performing small statistics calculations with ensemble S_1, we verified that overlap low-mode abundances are reasonably stable in the vicinity of this value.

At fixed N_f, the mass m of degenerate quarks provides for the only parameter distinguishing various physical behaviors in this set of theories. At $N_f = 2$, there is valence spontaneous chiral symmetry breaking at arbitrary m, while at $N_f = 12$, there could be a transition to chirally symmetric vacuum when m is sufficiently small. The logic behind the choice of ensembles in Table 3 is that system S_1, characterized by larger mass, was found in Ref. [29] to be mode condensing (vSChSB) with respect to staggered Dirac operator, while the system represented by S_2 and S_3 appeared non-condensing (valence chiral symmetry) at this cutoff. Note that S_2 and S_3 only differ by volume to give a sense of finite-volume effects.

4.2. Selected results

We now proceed to discuss the results from the perspective of vSChSB–ChP correspondence. Our extensive treatment of formalism in Section 2 and analysis of finite-temperature data in Section 3 served in part to identify effective ways to perform a study of this type. Here we show the raw data for C_A vs. λ, together with the plots of $\sigma_{ch}(\sigma)$, $\rho(\lambda)$, and $P_A(X, \sigma \to 0)$. The former three are designed to reveal whether vSChSB and ChP are tied together, while the latter serves as a first step to explore the newly proposed convexity connections in this particular corner of quark–gluon dynamics.

Fig. 18 shows the above set of characteristics for the system at larger of the two quark masses, represented by ensemble S_1. A mere glance at the raw data (top left) reveals the presence of chiral polarization at low energy without noticeable depletion of eigenvalues near the origin. The system thus shows simultaneous signs of chiral polarization and mode condensation in accordance with vSChSB–ChP correspondence. This is confirmed by the behavior of $\sigma_{ch}(\sigma)$ (top right) and $\rho(\lambda)$ (bottom left). Indeed, the former shows the positive bump at low σ, characteristic of chiral polarization, while the behavior in the latter is typical of mode-condensing theory.

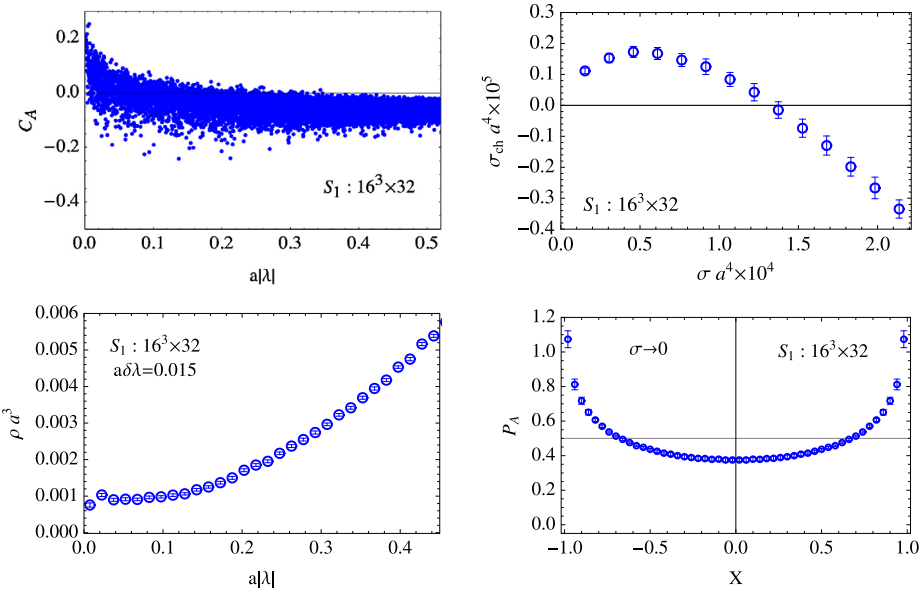

Fig. 18. Chiral polarization characteristics for ensemble S_1. See the discussion in the text.

Focusing now on the situation at smaller mass, the same set of characteristics are shown in Fig. 19, with the smaller volume (S_3) in the left column and the larger volume (S_2) in the right column. From the raw data alone (top row) one can immediately see that a qualitative change in the Dirac spectrum indeed occurred. However, it is not a simple depletion of eigenvalues in the vicinity of the origin as one would naively expect. Rather, there is a break in the spectrum, characterized by significant depletion, together with the accumulation of modes very close to zero. Given that, vSChSB–ChP correspondence predicts chiral polarization at the low end of the spectrum. This is indeed featured in the raw data qualitatively, and is properly quantified via the behavior of $\sigma_{ch}(\sigma)$ (second row).

While the options are limited for finite-volume scaling with only two volumes available, there is little doubt that the theory in question is overlap mode condensing. Indeed, as one can see in the third row of Fig. 19, the peak in the density near the origin is actually growing as the volume is increased. On the chiral polarization side, the positive maximum in $\sigma_{ch}(\sigma)$, namely Ω_{ch}, visibly shrinks at larger volume. Thus, a detailed finite volume study is required to decide whether the infinite-volume correspondence in the form of Conjecture 2 or Conjecture 2′ holds true. However, the position of the maximum in $\sigma_{ch}(\sigma)$, namely Ω, in fact mildly increases. We thus expect that the correspondence in the form of Conjecture 2″ certainly holds in this case. Needless to say, our results are also in agreement with chiral polarization characteristics being the finite-volume order parameters of vSChSB, and thus concur with Conjectures 3, 3′.

Lastly, we comment on the behavior of absolute X-distributions for lowest modes, i.e. $P_A(X, \sigma \to 0)$. These results are shown in the lower right plot of Fig. 18 and the last row of Fig. 19. Only the lowest 15 modes from each ensemble were used in the computation, leading to coarse-graining parameter $\Delta \ll \Omega$ in each case. All three systems exhibit convex behavior, thus following the same pattern observed in case of $N_f = 0$ at finite temperature for chirally polarized theories ($T < T_{ch}$). It should be mentioned here that the same holds for the $N_f = 2 + 1$ systems

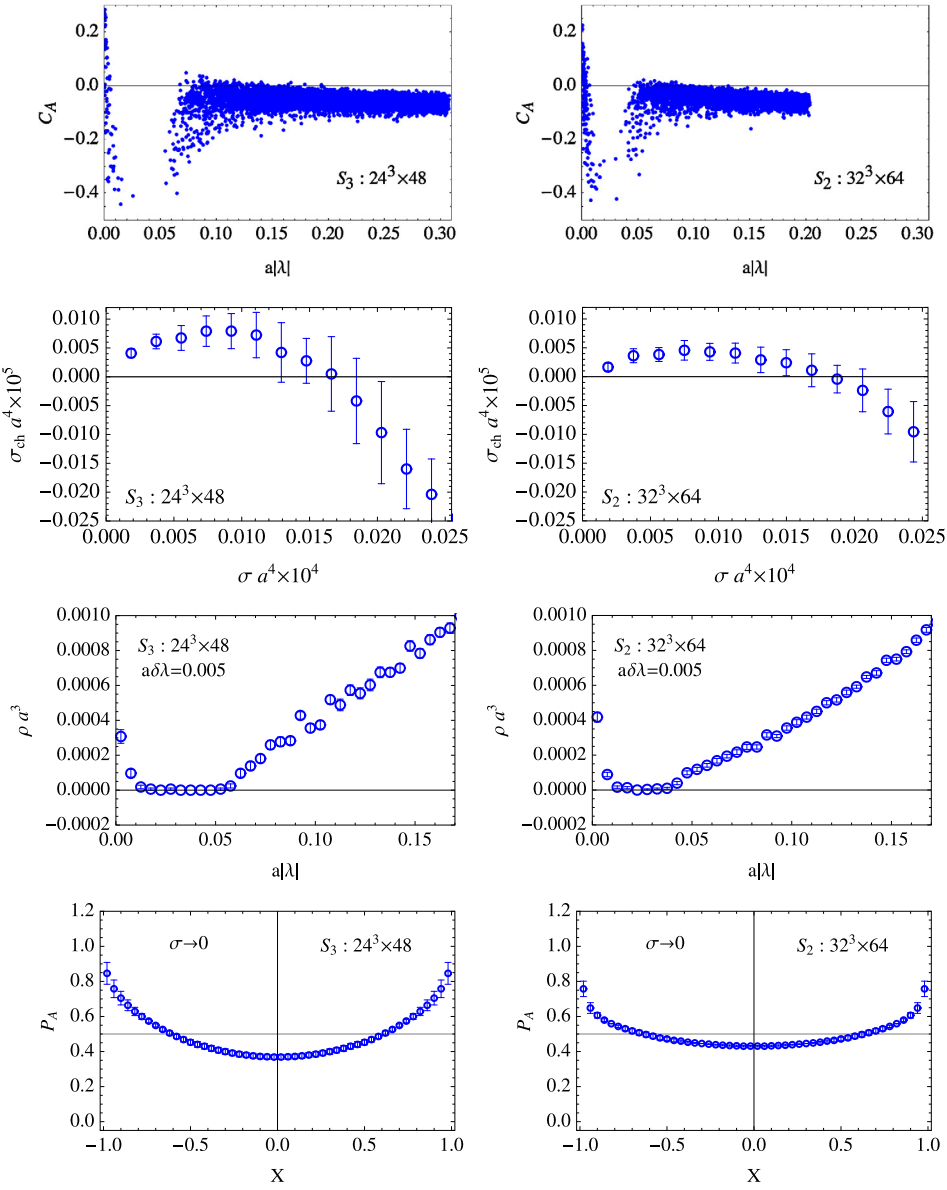

Fig. 19. Chiral polarization characteristics for ensemble S_2 (right column) and S_3 (left column). See the discussion in the text.

close to "real world QCD" studied in Ref. [3]. It is thus reasonable to expect that vSChSB is equivalent to convexity of $P_A(X, \sigma \to 0)$ over the whole base set $\mathcal{T}$.

4.3. Intermediate phases

The above discussion of finite-temperature and many-flavor results evokes certain analogy between the mixed phase in $N_f = 0$ QCD and the situation found in $N_f = 12$ at lighter mass

(ensembles S_2 and S_3). It appears that decreasing quark mass for $N_f = 12$ has a dynamical effect similar to increasing temperature for $N_f = 0$ in that a phase with narrow band of near-zeromodes separated from the bulk is generated, at least for certain range of cutoffs. In thermal case, the onset of this behavior appears to coincide with deconfinement, and thus T_c. In many-flavor case, where confinement is non-trivial to define, there is presumably a mass m_{in} below which this starts occurring.[12] Regardless of whether the existence of m_{in} is a lattice artifact, we can define an analog of T_{ch}, namely m_{ch}, below which valence chiral symmetry gets restored in $N_f = 12$. The aforementioned analogy would then apply to the regime $T_c < T < T_{ch}$ of $N_f = 0$ and $m_{ch} < m < m_{in}$ of $N_f = 12$, which we refer to as "intermediate phases" in what follows. It should be emphasized that whether m_{ch} is zero or non-zero is currently an open issue.

In what follows we summarize few observations on the two intermediate phases and compare them. Given that the available data on the many-flavor side is rather limited, this should be considered an initial assessment which can serve as a starting point for more detailed investigation.

(i) *Separation from the bulk*. Both intermediate phases are characterized by anomalous behavior of spectral density $\rho(\lambda)$, wherein the narrow peak forms near the origin, and is clearly distinguished from the rest of the spectrum. This is "anomalous" in the sense that, by virtue of the above, $\rho(\lambda)$ becomes non-monotonic. Note that in the thermal case, data indicates that the peak of near-zeromodes becomes of δ–function type in the infinite volume limit while it is currently not clear what happens in $N_f = 12$.

(ii) *Inhomogeneity*. The anomalous near-zeromodes are highly inhomogeneous in both intermediate phases. By this we mean that the bulk of their norm is carried by very small fraction of space–time points. Here we will not focus on quantifying this feature, but it will certainly become a characteristic of interest if either one of the intermediate phases turns out to be the reality of the continuum limit.

(iii) *Indefinite convexity*. As discussed in Sections 3.5, 3.6, thermal transition to intermediate (mixed) phase in $N_f = 0$ is characterized by the appearance of modes with indefinite convexity of absolute X-distributions. In case of $N_f = 12$ we do not find a clear evidence of this happening. In fact, the spectral transition from chirally polarized to chirally anti-polarized regime looks more like a direct transition from strictly convex to strictly concave distribution. In Fig. 20 (left column) we show $P_A(X, \sigma)$ for $\sigma \approx \Omega$. As one can see both for heavier mass (top) and the lighter mass in intermediate phase (bottom), the absolute X-distribution is flat which is characteristic of the direct transition. The right column in the figure illustrates the concave behavior at larger values of σ. Thus, to the extent that indefinite convexity of P_A reflects deconfinement even in the situation with light dynamical quarks, the intermediate phase in $N_f = 12$ exhibits not only valence chiral symmetry breaking but also signs of confinement. Detailed inquiry at yet lower mass should clarify this further.

5. Discussion

The main purpose of this work is to test the idea that, for quark–gluon interactions of QCD type, generating chiral condensate is the same thing as generating the layer of chirally polarized Dirac eigenmodes at low end of the spectrum [3]. When viewed as a feature characterizing

[12] If this behavior survives the continuum limit, then some universal parametrization of the transition point e.g. in terms of ratios of certain hadron masses, will be more appropriate. The same applies to m_{ch}.

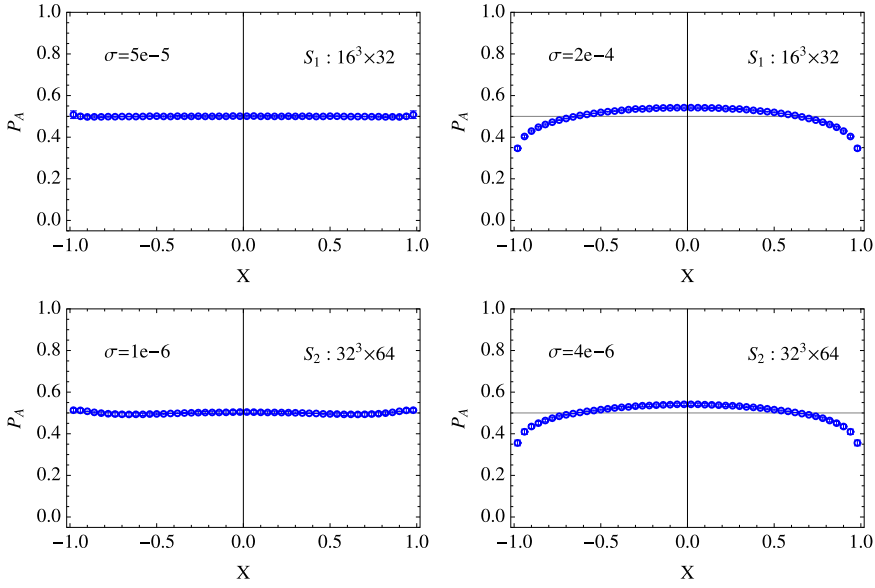

Fig. 20. Absolute X-distributions $P_A(X,\sigma)$ for ensemble S_1 (top) and S_2 (bottom). In the left column $\sigma \approx \Omega$ while in the right column $\sigma > \Omega$. Coarse-graining parameter $\delta = 10^{-5}$ was used for S_1 and $\delta = 2 \times 10^{-7}$ for S_2.

the state of vacuum correlations, this connection is not limited to theories containing massless quarks, but applies generically, even when all quarks are massive. In such generalized context, vacuum correlations are probed by a pair of external (valence) massless quarks and the role of chiral symmetry breaking is assumed by its valence counterpart. Examining the temperature effects in $N_f = 0$ QCD, and effects of many light flavors at $T = 0$ (for $N_f = 12$), we find a complete agreement with this vSChSB–ChP correspondence.

One relevant aspect of this connection, both practically and conceptually, is that it is perfectly well-defined even at lattice-regularized level. Indeed, if lattice fermions with exact chiral symmetry provide the massless probe, then vSChSB has a full-fledged lattice representation.[13] The associated conjectures can then be formulated directly for lattice theories, as done here, but with compliance only expected sufficiently close to the continuum limit. Nevertheless, we found the agreement for every lattice system studied, even in corners where relevance for continuum physics hasn't yet been established, e.g. in the "mixed phase" of $N_f = 0$ QCD. It is thus conceivable that the connection is even more robust than originally expected.

Important motivation to identify the correspondence of vSChSB–ChP type is to narrow down options in searches for specific mechanism of the breaking phenomenon. Indeed, the two aspects involved are not required to be locked together by general principles and are in fact quite different in nature. Like that of any broken symmetry, the definition of vSChSB is intimately tied to thermodynamic limit (infinite volume). On the other hand, ChP is defined in any fixed finite volume which is quite natural given its role to characterize and detect chiral symmetry breaking nature of the interaction at hand. Indeed, such indicator is not expected to turn itself on in infinite volume only, but rather when volume is sufficiently large to contain relevant finite scales of the theory.

[13] ChP is in fact well-defined even if probing fermion is not exactly chiral away from continuum limit.

Above considerations lead to the notion of *finite-volume "order parameter"* introduced in Section 2.4. This is intended to be a dynamical quantifier assuming non-zero value in sufficiently large *finite* volumes if and only if the symmetry in question is broken (in infinite volume). The width of chiral polarization layer (Λ_{ch}), the volume density of total chirality (Ω_{ch}), and the volume density of polarized modes (Ω), are viewed as prototypes of such objects associated with vSChSB (see Conjectures 3, 3′), and all available data is consistent with this proposition. In fact, we have not yet encountered a reversal of dynamical tendency for chiral polarization due to the volume being too small. In this vein, it is instructive to think of chiral polarization framework as an attempt to construct a "predictor" of valence chiral symmetry breaking for QCD-like theories. Such predictor, say Ω, will be most efficient if it is also a finite-volume order parameter. Indeed, a well-founded wager on vSChSB can then be made based on the value of Ω in a single otherwise acceptable volume.

Conceptual simplicity in the notion of finite-volume order parameter is further underlined by the fact that all three ChP–based characteristics are (non)zero simultaneously in finite volume. Thus, although the state of chiral polarization is characterized by the triplet

$$\mathrm{ChP}_{V<\infty} \;\longleftrightarrow\; \big(\Lambda_{ch}(V), \Omega_{ch}(V), \Omega(V)\big) \tag{28}$$

the associated vSChSB inquiry in fact involves a single object, namely

$$\chi_p(V) \equiv \mathrm{sgn}\big(\Lambda_{ch}(V)\big) = \mathrm{sgn}\big(\Omega_{ch}(V)\big) = \mathrm{sgn}\big(\Omega(V)\big) \in \{0, 1\} \tag{29}$$

Note that, as finite-volume order parameters, elements of $\mathrm{ChP}_{V<\infty}$ are not required to have non-zero infinite-volume limits when symmetry is broken, but $\chi_p \equiv \lim_{V\to\infty} \chi_p(V) = 1$.

If, contrary to initial evidence, the notion of finite-volume order parameter on $\mathcal{T}$ doesn't materialize, vSChSB–ChP correspondence can still be based on order parameters of more traditional variety: those indicating the symmetry breakdown by positive *infinite-volume* value. The situation becomes more structured though, since the classification of possible ChP behaviors in infinite volume is given by the heptaplet of non-negative parameters

$$\mathrm{ChP}_{V=\infty} \;\longleftrightarrow\; \big(\Lambda_{ch}, \Lambda_{ch}^{\infty}, \Omega_{ch}, \Omega_{ch}^{\infty}, \Omega, \Omega^{\infty}, \chi_p\big) \tag{30}$$

with variety of mixed-positivity scenarios allowed in principle. In this language, the hypothetical lack of finite-volume order parameter implies that χ_p is not a good infinite-volume indicator of vSChSB. Nevertheless, in the vSChSB–ChP correspondence being constructed, $\chi_p = 0$ still indicates symmetric vacuum since it implies vanishing of all elements in $\mathrm{ChP}_{V=\infty}$ and thus absence of any polarized behavior. However, to formulate the equivalence, one needs to specify which forms of $\mathrm{ChP}_{V=\infty}$ with $\chi_p = 1$ are associated with vSChSB. This heavily depends on the scope of polarized behaviors generated by theories in $\mathcal{T}$.

To this effect, we formulated three versions of such infinite-volume correspondence that are not mutually exclusive, but include an increasingly large variety of chiral polarization. The most restrictive form, Conjecture 2, assumes that no singular cases occur sufficiently close to the continuum limit [3]. Here "singular" refers to any combination of the first six elements in $\mathrm{ChP}_{V=\infty}$ with mixed positivity, or with paired characteristics not matching (e.g. $\Lambda_{ch} \neq \Lambda_{ch}^{\infty}$). In this case, each element of $\mathrm{ChP}_{V=\infty}$ (except χ_p) is individually a valid infinite-volume order parameter of vSChSB. Such scenario was only found to be violated in the narrow mixed phase of $N_f = 0$ QCD, but complete agreement may hold closer to continuum limit, which is sufficient. In Conjecture 2′ we minimally expanded the range of anticipated ChP behaviors in order to include the singular option encountered above, namely $\Lambda_{ch} = \Lambda_{ch}^{\infty} = 0$ and $0 < \Omega_{ch} < \Omega$. Here Ω_{ch}, Ω and

their partners are each an infinite-volume order parameter of vSChSB. Most generally, Conjecture 2″ admits all singular ChP behaviors, in which case Ω becomes the sole reliable indicator of vSChSB: the layer of chirally polarized modes is expected to be physically relevant only when total volume density of participating modes remains positive in the infinite-volume limit.

We emphasize that having differently focused versions of vSChSB–ChP correspondence simply reflects differently aimed benefits of the underlying relationship. Indeed, the more restrictive the form of correspondence turns out to be valid, the more information on the continuum behavior of vSChSB it conveys. On the other hand, the more generic the formulation becomes, the wider its applicability becomes in terms of cutoff theories. In an extreme case, the relationship might turn out to be as generic as the vSChSB–QMC correspondence, i.e. valid at arbitrary non-zero cutoff.

The analysis in this paper (and the discussion above) focuses attention to Ω as a central characteristic of ChP in relation to vSChSB. Indeed, not only does Ω provide for the simple and most generic way to express vSChSB–ChP correspondence, it is also expected to be a universal quantity characterizing QCD vacuum (see Section 2.5). Moreover, our numerical experiments show that the most practical scheme for detecting chiral polarization proceeds via computing the dependence of σ_{ch} on σ, from which Ω (and Ω_{ch}) is directly determined.

During the course of our main inquiry we encountered few results that are noteworthy in their own right. The first one relates to the issue of thermal mixed phase ($T_c < T < T_{ch}$) in $N_f = 0$ QCD, i.e. the existence of deconfined system in real Polyakov line vacuum but with broken valence chiral symmetry [14]. This is a well-posed and interesting question even at given cutoff, but its resolution requires a careful volume study. Our data involves several volumes and the results indicate that the mixed phase with overlap valence quarks does indeed exist, at least for some range of cutoffs. The associated vSChSB proceeds via band of spatially inhomogeneous and chirally polarized near-zeromodes, well separated from the rest of the spectrum. The width of the band appears to vanish in the infinite-volume limit, possibly involving $\delta(\lambda)$ singularity in spectral density. We found that a similar phase also exists in $N_f = 12$ theory at light quark mass, which deserves a dedicated study.

The last side result we wish to discuss suggests novel characterization of (de)confinement. While at $T < T_c$ only convex or concave absolute X-distributions of Dirac modes are found in $N_f = 0$ QCD, the band of convex-indefinite modes appears at $T > T_c$. Thus, at least in this setting, the existence of such band seems to play the same role for deconfinement as the existence of chirally polarized band plays for vSChSB. Both layers are present in the mixed phase as they should. The situation at high temperatures brings up an interesting question, namely how does the "concavity edge", marking the transition from convex-indefinite to concave behavior in Dirac spectra at $T > T_c$, relate to "mobility edge" feature discussed in Refs. [22–24]? With natural expectation being the coincidence of the associated scales, computations needed to explore this issue are straightforward to set up.

Acknowledgements

We are indebted to Anna Hasenfratz and David Schaich for sharing their $N_f = 12$ staggered fermion configurations for the purposes of this work. Thanks to Terry Draper for discussions, and to Mingyang Sun for help with graphics. A.A. is supported by U.S. National Science Foundation under CAREER grant PHY-1151648. I.H. acknowledges the support by Department of Anesthesiology at the University of Kentucky.

Appendix A. Absolute polarization and dynamical chirality

In this appendix we briefly describe the absolute (dynamical) polarization method of Ref. [4]. In the present context the elementary object of study is a chirally decomposed eigenmode $\psi = \psi_L + \psi_R$. Given that we are only interested in local (on-site) relationship between left and right, the sufficient information is stored in the probability distribution $\mathcal{P}_f(\psi_L, \psi_R)$ of its values $(\psi_L(x), \psi_R(x))$. This setup coincides with the starting point of a general approach that considers arbitrary stochastic quantity Q with values in a vector space decomposed into a pair of equivalent orthogonal subspaces ($Q = Q_1 + Q_2$, $Q_1 \cdot Q_2 = 0$), and whose "dynamics" is described by symmetric probability distribution $\mathcal{P}_f(Q_1, Q_2) = \mathcal{P}_f(Q_2, Q_1)$.

Given the goal of characterizing the (normalized) asymmetry between the two subspaces in favored values of Q (polarization), the method proceeds by first marginalizing the full distribution $\mathcal{P}_f(Q_1, Q_2)$ to the distribution of magnitudes $\mathcal{P}_b(q_1, q_2)$. Indeed, the weight of a given subspace in sample Q can be assessed via magnitude $q_i \equiv |Q_i|$ of its component. One possibility for a normalized variable expressing the desired relationship is [7]

$$x = \frac{4}{\pi} \tan^{-1}\left(\frac{q_2}{q_1}\right) - 1 \equiv \mathcal{X}_r(q_1, q_2) \tag{31}$$

namely the *reference polarization coordinate*. Note that $x \in [-1, 1]$ with extremal values taken by samples strictly polarized into one of the subspaces, and zero value assigned to strictly unpolarized samples ($q_1 = q_2$). Probability distribution of x in $\mathcal{P}_b(q_1, q_2)$, namely

$$P_r(x) = \int_0^\infty dq_1 \int_0^\infty dq_2 \mathcal{P}_b(q_1, q_2) \delta\big(x - \mathcal{X}_r(q_1, q_2)\big) \tag{32}$$

is called the *reference X-distribution*, and represents detailed polarization characteristic of dynamics $\mathcal{P}_f(Q_1, Q_2)$ with respect to polarization measure $\mathcal{X}_r$.

The large freedom in choosing the polarization measure makes the above characteristic highly non-unique and thus kinematic. Various "reference frames" of polarization can be represented by suitably constructed *polarization functions* $\mathcal{X}(x)$. In this language, the reference X-distribution is associated with polarization function $\mathcal{X}_r(x) = x$. The main idea driving the absolute polarization method is to adjust the polarization function characterizing $\mathcal{P}_b(q_1, q_2)$ so that it measures polarization relative to its "own statistical independence", namely relative to the stochastic dynamics described by

$$\mathcal{P}_b^u(q_1, q_2) \equiv p(q_1) p(q_2) \qquad p(q) \equiv \int_0^\infty dq_2 \mathcal{P}_b(q, q_2) = \int_0^\infty dq_1 \mathcal{P}_b(q_1, q) \tag{33}$$

One can show [4] that this is accomplished by utilizing the polarization function

$$\mathcal{X}_A(x) \equiv 2 \int_{-1}^{x} dy P_r^u(y) - 1 \tag{34}$$

where reference X-distribution $P_r^u(x)$ is associated with uncorrelated dynamics $\mathcal{P}_b^u(q_1, q_2)$. The corresponding distribution of polarization values, namely

$$P_A(X) \equiv \int_{-1}^{1} dx\, P_r(x)\delta\big(X - \mathcal{X}_A(x)\big) = \frac{1}{2}\frac{P_r(\mathcal{X}_A^{-1}(X))}{P_r^u(\mathcal{X}_A^{-1}(X))} \tag{35}$$

is called the *absolute X-distribution*. By construction, and as seen from the above explicit form, $P_A(X)$ is a differential measure quantifying polarization tendencies relative to statistical independence. Moreover, it is unique: arbitrary choice of the reference polarization coordinate (function) leads to the same absolute X-distribution [4].[14] Consequently, absolute X-distribution is viewed as a genuinely dynamical concept.

Differential information contained in $P_A(X)$ can be integrated into the *correlation coefficient of polarization* $C_A \in [-1, 1]$, namely

$$C_A \equiv 2\int_{-1}^{1} dX|X|P_A(X) - 1 \tag{36}$$

Statistical meaning of C_A is clarified by noting that the integral in the above expression is the probability for sample drawn from $\mathcal{P}_b(q_1, q_2)$ to be more polarized than sample drawn from $\mathcal{P}_b^u(q_1, q_2)$. Consequently, positive correlation means that stochastic dynamics enhances polarization relative to statistical independence, while negative correlation (anti-correlation) implies its suppression. $\mathcal{P}_f(Q_1, Q_2)$ is said to support *dynamical polarization* in the former case and *dynamical anti-polarization* in the latter. In the context of Dirac eigenmodes and their chiral decomposition, expressions like "mode is chirally polarized" vs. "anti-polarized", "mode is chirally correlated" vs. "anti-correlated", or "mode supports dynamical chirality" vs. "anti-chirality", are all verbal descriptions of $C_A > 0$ vs. $C_A < 0$.

Appendix B. Generalities on spectral definitions

The primary entities involved in spectral definitions are the cumulative densities $\sigma(\lambda)$ and $\sigma_{ch}(\lambda)$. At the regularized level, σ is proportional to certain cumulative probability function of λ (non-decreasing, bounded) and can thus have at most countably many finite discontinuities. All of its possible behaviors are then contained in the form

$$\sigma(\lambda, M, V) = \sum_j A_j H(\lambda - \alpha_j) + \hat{\sigma}(\lambda, M, V) \tag{37}$$

where $\alpha_j = \alpha_j(M, V) \geq 0$ are the points of discontinuity, $A_j = A_j(M, V) \geq 0$, and $H(x)$ is the left-continuous version of the Heaviside step function ($H(x) = 0$ for $x \leq 0$ and $H(x) = 1$ for $x > 0$). $\hat{\sigma}$ is a continuous non-decreasing function of λ and, as such, it can only be non-differentiable on the set of Lebesgue measure zero. However, the exotic "Cantor function"-like cases, where the subset of non-differentiability is uncountable, are very unlikely to appear in this physical context. Differentiable functions producing derivatives that are discontinuous on uncountable subsets can be quite safely omitted for the same reason. Thus, the "standard model" of cumulative mode density, expected to cover all theories considered, is (37) with $\hat{\sigma}(\lambda)$ being a continuous non-decreasing function that is continuously differentiable except for countably many (thus isolated) points. The differential representation (generalized function) then exists and is given by

[14] This uniqueness of the "correlational" approach is in fact why the method is referred to as *absolute*.

$$\bar{\rho}(\lambda, M, V) = \sum_j A_j \delta(\lambda - \alpha_j) + \hat{\rho}(\lambda, M, V) \tag{38}$$

where the ordinary function $\hat{\rho}(\lambda) = d\hat{\sigma}(\lambda)/d_+\lambda$ exists and is continuous except for points $a_k = a_k(M, V) \geq 0$ where it can have an integrable divergence or simple discontinuity. Note that there is no a priori relation between sets $\{\alpha_j\}$ and $\{a_k\}$.

The definition of cumulative chirality density is a priori less constraining on its behavior. Indeed, while $\sigma_{ch}(\lambda)$ is bounded in absolute value by $\sigma(\lambda)$, it is not necessarily monotonic, and the most general form analogous to (37) is thus not strictly guaranteed. On the other hand, more singular behavior of $\sigma_{ch}(\lambda)$ would require $C_A(\lambda)$ – a dynamical property – to be discontinuous on uncountable subsets which is highly unlikely in this physical setting. Thus, the most general form of $\sigma_{ch}(\lambda)$ expected to occur is

$$\sigma_{ch}(\lambda, M, V) = \sum_j B_j H(\lambda - \beta_j) + \hat{\sigma}_{ch}(\lambda, M, V) \tag{39}$$

where $B_j = B_j(M, V)$ has indefinite sign, $\beta_j = \beta_j(M, V) \geq 0$, and $\hat{\sigma}_{ch}$ is a continuous function of λ. In slightly more restrictive "standard model", guaranteeing differential representation, $\hat{\sigma}_{ch}(\lambda)$ is also continuously differentiable except for countably many points, i.e.

$$\bar{\rho}_{ch}(\lambda, M, V) = \sum_j B_j \delta(\lambda - \beta_j) + \hat{\rho}_{ch}(\lambda, M, V) \tag{40}$$

The function $\hat{\rho}_{ch}(\lambda) = d\hat{\sigma}_{ch}(\lambda)/d_+\lambda$ exists and is continuous everywhere except for points $b_k = b_k(M, V) \geq 0$ where it can have an integrable divergence or a simple discontinuity. Note that the sets $\{\beta_j\} \subseteq \{\alpha_j\}$ need not be identical, and neither do the sets $\{a_k\}$, $\{b_k\}$.

There is very little doubt that the behavior of $\sigma(\lambda)$ and $\sigma_{ch}(\lambda)$ in all theories considered falls under the "standard model" description specified above. In fact, it appears very likely that only more restricted forms will actually appear. Nevertheless, it is interesting to note that the key concepts utilized in our discussion, namely that of chiral polarization scale Λ_{ch} and low-energy chirality Ω_{ch}, are well-defined without any assumptions placed on $\sigma_{ch}(\lambda)$ beyond its existence. More precisely, below we put forward definitions that assign definite characteristics to any real-valued function $\sigma_{ch}(\lambda)$ such that $\sigma_{ch}(\lambda) \equiv 0$ for $\lambda \leq 0$, and bounded on any $(-\infty, \Lambda]$.

We first define Λ_{ch} as the "largest" Λ, such that $\sigma_{ch}(\lambda)$ is strictly increasing on $[0, \Lambda]$, i.e.

$$\Lambda_{ch}[\sigma_{ch}] \equiv \sup\left\{\Lambda \;\middle|\; \sigma_{ch}(\lambda_1) < \sigma_{ch}(\lambda_2) \text{ for all } 0 \leq \lambda_1 < \lambda_2 \leq \Lambda\right\} \tag{41}$$

when σ_{ch} is not strictly increasing on $[0, \infty)$, and $\Lambda_{ch} = \infty$ otherwise. Note that when positive Λ_{ch} doesn't exist, the defining condition (41) is vacuously satisfied by $\Lambda_{ch} = 0$ which is then its assigned value. Thus, $\Lambda_{ch}[\sigma_{ch}]$ always exists and is non-negative.

Next, associate with $\sigma_{ch}(\lambda)$ its "running maximum function"

$$\sigma_{ch}^m(\lambda) \equiv \sup\left\{\sigma_{ch}(\lambda') \;\middle|\; \lambda' \leq \lambda\right\} \tag{42}$$

which is a non-negative non-decreasing function bounded on any $(-\infty, \Lambda]$. Thus, it can only be discontinuous via countably many finite jumps, and one-sided limits exist everywhere. The low-energy chiral polarization is then defined as

$$\Omega_{ch}[\sigma_{ch}] \equiv \lim_{\lambda \to \Lambda_{ch}^+} \sigma_{ch}^m(\lambda) \tag{43}$$

We emphasize that the above definitions of Λ_{ch} and Ω_{ch} coincide with those given in the main text when $\sigma_{ch}(\lambda)$ is of "standard form".

References

[1] T. Banks, A. Casher, Nucl. Phys. B 169 (1980) 125.
[2] A. Morel, J. Phys. (Paris) 48 (1987) 1111.
[3] A. Alexandru, I. Horváth, Phys. Lett. B 722 (2013) 160, arXiv:1210.7849.
[4] A. Alexandru, T. Draper, I. Horváth, T. Streuer, Ann. Phys. 326 (2011) 1941, arXiv:1009.4451.
[5] H. Neuberger, Phys. Lett. B 417 (1998) 141;
H. Neuberger, Phys. Lett. B 427 (1998) 353.
[6] S. Chandrasekharan, Phys. Rev. D 60 (1999) 074503, arXiv:hep-lat/9805015.
[7] I. Horváth, N. Isgur, J. McCune, H.B. Thacker, Phys. Rev. D 65 (2002) 014502, arXiv:hep-lat/0102003.
[8] D. Comelli, M. Pietroni, Phys. Lett. B 417 (1998) 337, arXiv:hep-ph/9708489.
[9] J. Braun, H. Gies, Phys. Lett. B 645 (2007) 53, arXiv:hep-ph/0512085.
[10] L. Del Debbio, et al., J. High Energy Phys. 0602 (2006) 011, arXiv:hep-lat/0512021.
[11] L. Giusti, S. Necco, J. High Energy Phys. 0704 (2007) 090, arXiv:hep-lat/0702013.
[12] A. Alexandru, I. Horváth, PoS Lattice 2012 (2012) 210, arXiv:1211.2601.
[13] A. Alexandru, I. Horváth, J. Phys. Conf. Ser. 432 (2013) 012034, arXiv:1211.3728.
[14] R.G. Edwards, U.M. Heller, J.E. Kiskis, R. Narayanan, Phys. Rev. D 61 (2000) 074504, arXiv:hep-lat/9910041.
[15] ALPHA Collaboration, M. Guagnelli, R. Sommer, H. Wittig, Nucl. Phys. B 535 (1998) 389, arXiv:hep-lat/9806005.
[16] A.M. Polyakov, Phys. Lett. B 72 (1978) 477.
[17] B. Svetitsky, L.G. Yaffe, Nucl. Phys. B 210 [FS6] (1982) 423.
[18] S. Chandrasekharan, N. Christ, Nucl. Phys. B, Proc. Suppl. 47 (1996) 527, arXiv:hep-lat/9509095.
[19] C. Gattringer, P.E.L. Rakow, A. Schafer, W. Soldner, Phys. Rev. D 66 (2002) 054502, arXiv:hep-lat/0202009.
[20] T. Kovács, PoS LAT2008 (2008) 198, arXiv:0810.4763.
[21] F. Karsch, Nucl. Phys. B, Proc. Suppl. 60A (1998) 169, arXiv:hep-lat/9706006.
[22] A.M. Garcia-Garcia, J.C. Osborn, Phys. Rev. D 75 (2007) 034503, arXiv:hep-lat/0611019.
[23] T. Kovács, F. Pitler, Phys. Rev. Lett. 105 (2010) 192001, arXiv:1006.1205.
[24] T. Kovács, F. Pitler, Phys. Rev. D 86 (2012) 114515, arXiv:1208.3475.
[25] T. Banks, A. Zaks, Nucl. Phys. B 196 (1982) 189.
[26] E. Neil, PoS Lattice 2011 (2011) 009, arXiv:1205.4706.
[27] J. Giedt, PoS Lattice 2012 (2012) 006.
[28] E. Itou, in: Proceedings of the 31st International Symposium on Lattice Field Theory, July 29–August 3, Mainz, Germany, 2013, arXiv:1311.2676.
[29] A. Hasenfratz, A. Cheng, G. Petropoulos, D. Schaich, PoS Lattice 2012 (2012) 034, arXiv:1207.7162.
[30] A. Cheng, A. Hasenfratz, D. Schaich, Phys. Rev. D 85 (2012) 094509, arXiv:1111.2317.